Using lipidomics to investigate the predator-prey dynamics of *Emiliania huxleyi* and *Oxyrrhis marina*

by

Elizabeth Baldo

A Thesis Presented
In Partial Fulfillment for the Requirements of the
Master of Science

Under the Supervision of
Dr. Kelsey Poulson-Ellestad

Roosevelt University
College of Science, Health and Pharmacy
Department of Biological, Physical and Health Sciences

Submitted: October 23, 2022

List of Abbreviations

BL	betaine lipid
BLL	betaine-like lipid
Chl	chlorophyll
DAG	diacylglycerol
DGCC	diacylglycerol carboxymethylcholine
DGDG	digalactosyldiacylglycerol
FFA	free fatty acid
Fuco	fucolipid
LPA	lipoprotein(a)
MAG	monoacylglycerol
MGDG	monogalactosyldiacylglycerol
OPLS-DA	orthogonal partial least squares discriminant analysis
PA	phosphatidic acid
PC	phosphatidylcholine
PCA	principal component analysis
PDM	peridroplet mitochondria
PDPT	phosphatidyldimethylpropanethiol
PE	phosphatidylethanolamine
PG	phosphatidylglycerol
PLS-DA	partial least squares discriminant analysis
PLSR	partial least squares regression
PQ	plastoquinone
PS	phosphatidylserine
PUA	polyunsaturated aldehyde
PUFA	polyunsaturated fatty acid
SQDG	sulfoquinovosyldiacylglycerol
TAG	triacylglycerol
UQ	ubiquinone
WE	wax ester

ABSTRACT

My thesis work explored the rich variation present in the lipidomes of the coccolithophore *Emiliania huxleyi* and the dinoflagellate *Oxyrrhis marina*. Interactions between single-cell marine predators and their prey are complex, and lipidomics analysis is a useful tool for exploring this dynamic. Using PCA and presence/absence analysis, I investigated how the lipid makeup of these two organisms changes due to differences in genotype and phenotype, as well as in response to grazing. Specifically, I identified lipid classes and individual lipids in *E. huxleyi* indicative of calcification state, ploidy level, and grazer exposure. In *O. marina*, I identified lipid classes and individual lipids indicative of a fed state. I found that *E. huxleyi* lipidomes differ based on calcification state and ploidy level and have both shared and strain-specific responses to grazing stress. I found that the *O. marina* lipidome undergoes both general changes upon feeding, as well as changes unique to consuming specific strains of *E. huxleyi*. Given how vital phytoplankton are to the marine ecosystem, and the oversized effect that protist grazers have on phytoplankton populations, increasing our understanding of the predator-prey dynamics between these two groups of organisms is of the utmost importance.

INTRODUCTION

Phytoplankton are incredibly important members of the marine ecosystem. Through photosynthesis, they account for half of the primary productivity on planet Earth, and half of all oxygen production (Field et al., 1998). Phytoplankton also serve as the base of the oceanic food web. Their numbers are primarily controlled by sunlight, dissolved nutrients, viral infection, and grazing. Coccolithophores are single-celled, photosynthetic eukaryotes, which are known for possessing a layered coating of calcium carbonate plates called coccoliths (Monteiro et al.,

2016). Coccolithophores are a prominent member of the phytoplankton, with hundreds of known strains and many more likely undiscovered (Monteiro et al., 2016).

Emiliania huxleyi is one species of coccolithophore, also consisting of many different strains, which is widely used as a model organism for phytoplankton research. Some *E. huxleyi* strains exist in a naked (uncalcified) state while other strains possess various levels of calcification. A great deal is known about coccoliths and their composition (Monteiro et al., 2016), but little research has been done to explore what, if any, lipid biomarkers exist that can differentiate between a naked and calcified state. *E. huxleyi* can also exist in a haploid state or a diploid state. Haploid *E. huxleyi* are typically motile, naked, and resistant to viral infection, and diploid *E. huxleyi* are typically nonmotile, may be calcified or naked, and are susceptible to viral infection (Frada et al., 2008). While a good deal of research has been done that examines ploidy level and susceptibility to viral infection, there has been little research done that examines differences in the lipidomes of uninfected haploid and diploid *E. huxleyi*.

The calcium carbonate coccoliths present on calcified *E. huxleyi* and other coccolithophores play a unique role in the marine carbon cycle (Brownlee et al., 2015). Atmospheric CO_2 is absorbed by ocean waters via diffusion, and forms carbonic acid (H_2CO_3), as well as bicarbonate (HCO_3^-) and carbonate (CO_3^{2-}). Carbonate ions (CO_3^{2-}) in the ocean are used in the creation of coccoliths, and coccoliths then bring this carbon to the ocean floor when coccolithophores die (Brownlee et al., 2015). Through using carbon to build their coccoliths and then sequestering this carbon in the ocean floor upon their deaths, coccolithophores remove carbon from the water column. Due to the sheer number of calcified coccolithophores present in the ocean and the organism's ability to form enormous blooms, their impact on the carbon cycle

can be significant. Therefore, gaining understanding into what influences the population dynamics of these organisms is of great importance.

One prominent factor in the top-down control of phytoplankton, including coccolithophores, is grazing by protists, which can drastically reduce daily primary productivity (Calbet et al., 2013). Protist grazing is likely influenced by many factors in phytoplankton, including chemical, morphological, and behavioral features (Harvey et al., 2015). The protist grazer explored in this thesis, *Oxyrrhis marina*, is a heterotrophic dinoflagellate which is widely used as a model organism to study grazing behavior. *O. marina* consumes a huge variety of prey species via direct engulfment, and how the organism chooses between species, within a species, and what factors influence these choices are all very active fields of research (Roberts et al., 2011).

Previous research has found that *O. marina* is able to differentiate *E. huxleyi* cells based on strain identity and individual characteristics of cells within a strain. For instance, *O. marina* will select virally infected over non-virally infected *E. huxleyi* cells and can differentiate between *E. huxleyi* cells based on their DMSP activity (Roberts et al., 2011). One, as of yet, unexplored influencing factor involved in protist grazing is non-virally infected coccolithophore lipid composition. Lipids are extremely diverse in their form and function, and the specific makeup of these calorie-dense macromolecules in phytoplankton could influence predator growth and reproduction, and ultimately the population sizes of both grazers and phytoplankton.

One area of active research explores the impact of viral infection on coccolithophores (Sheyn et al., 2018). This research has looked at how different factors influence viral infection, such as calcification, ploidy level, and strain identity, as well as the effect that viral infection has on the transcriptome and lipidome (the complete collection of lipids in a cell or tissue type) of

infected coccolithophores. Another area of research that has no shortage of published works has to do with the impact of the fatty acid composition of algae on the fatty acid composition of copepod grazers, as copepods serve as a food source for many fish raised for human consumption (Pan et al., 2018).

We do not know how the lipidome of coccolithophores is influenced by grazing, and conversely, how the lipidome of coccolithophores influences grazing behaviors and the grazer lipidome. In this thesis, I investigated the relationship between lipid profiles and grazing pressure using *E. huxleyi* as a prey organism and *O. marina* as a protist grazer. I used lipidomic data obtained from samples collected during a previous experiment examining the impact of calcification in *E. huxleyi* on grazing by *O. marina* (Harvey et al., 2015). This previous study found that, while calcification could explain some of the variation in *O. marina* ingestion and growth rates when consuming different strains of *E. huxleyi*, calcification alone was not enough to predict these differences. This indicated that other factors aside from calcification were impacting predator-prey dynamics. One of those possible factors is *E. huxleyi* chemical composition. In the original experiment, researchers found that the rate at which *O. marina* ingested each *E. huxleyi* strain did not correspond to how quickly the *O. marina* grew while ingesting those strains (Table 1; see also Figs. 1A, 3A and 4 in Harvey et al., 2015), suggesting that not all strains are equally nutritious food sources.

Table 1. The four *Emiliania huxleyi* strains examined in this thesis. This information is taken from Harvey et al. (2015). Calcification state and ploidy level are listed for each strain. *Oxyrrhis marina* ingestion rate (pg C pred^{-1} day^{-1}) and growth rate (day^{-1}) are estimated using the graphs from Harvey et al. (2015) Figs. 1A and 3A, at a prey abundance of 700 ng C mL^{-1}. Grazing pressure refers to the combination of ingestion rate and growth rate across all prey abundances and their subsequent effect on *E. huxleyi* populations.

Emiliania huxleyi Strains Relevant Characteristics	379	374	624	607
Calcification State	Naked	Naked	Heavily Calcified	Lightly Calcified
Ploidy Level	1N	2N	2N	2N
O. marina* Ingestion Rate (pg C pred^{-1} day^{-1})	600	750	2,300	400
O. marina* Growth Rate* (day^{-1})	0.85	0.50	0.15	-0.15
Grazing Pressure	**High**	**Medium**	**Low**	**Extremely Low**

**Estimated from graph 1A in Harvey et al. (2015)*

***Estimated from graph 3A in Harvey et al. (2015)*

To account for the impact of both *O. marina* ingestion rate and growth rate on *E. huxleyi* populations over multiple prey concentrations, I have included my own term, grazing pressure (Table 1). Grazing pressure, as defined here, describes the overall strain-specific effects that *O. marina* has on *E. huxleyi* population size. For instance, strain 624 was grazed at a higher ingestion rate than the other three strains, however *O. marina* growth rates were extremely low when feeding on this strain. This resulted in much less top-down control from *O. marina* when feeding on strain 624 than would be indicated from looking at ingestion rate alone. Grazing pressure was greatest for strain 379, followed by strain 374, with strain 624 experiencing very low grazing pressure, and strain 607 experiencing the lowest grazing pressure of the four *E. huxleyi* strains (Table 1).

Collectively, these data indicate that both the attractiveness of each *E. huxleyi* strain to *O. marina* and the efficiency with which each strain can be digested and used for growth and reproduction in *O. marina* varies greatly among *E. huxleyi* strains. What modulates these differences are likely related to numerous characteristics of cells, including the lipid profiles of prey cells. To determine how the lipidomes of these organisms change in response to grazing

pressure, my thesis was divided into three main aims (Table 2). First, I examined the baseline lipidomes of the four *E. huxleyi* strains, to find lipid class trends and individual biomarkers indicative of calcification state and ploidy level, as well as lipids which were consistent across all four strains. Second, I examined the lipidomes of all four *E. huxleyi* strains after exposure to grazers, both individually and as a group to identify lipid class trends and individual lipid biomarkers indicative of stress. Third, I examined the lipidome of *O. marina* after consuming each individual *E. huxleyi* strain to assess how protist lipid composition varies depending upon food source. Together, these three goals open a window into how the *E. huxleyi* and *O. marina* lipidomes change in response to grazing, and they provide possible explanations for the grazing behavior trends observed in the Harvey et al. (2015) experiment. If confirmed experimentally, which is not within the scope of this thesis, the lipid biomarkers identified by my work could be used as clues to the state of predation in samples of *E. huxleyi* and *O. marina* taken from ocean waters. This would bring us one tiny step closer to understanding the incredibly intricate and dynamic predator-prey interactions that take place at the base of the marine food web.

Table 2. A summary of the analyses and findings described in this thesis.

	AIM I	AIM II	AIM III
Main Goal	**Exploration of *E. huxleyi* lipidome**	**Changes in *E. huxleyi* lipidome in response to grazer exposure**	**Changes in *O. marina* lipidome in response to feeding**
Lipids Analyzed	*E. huxleyi* control lipids	*E. huxleyi* grazed lipids	*O. marina* fed lipids
Main Comparison	• Naked vs. calcified • Haploid vs. diploid • Lipids common to all four strains	Control *E. huxleyi* vs. grazer exposed *E. huxleyi*	Unfed *O. marina* vs. fed *O. marina*
Findings	Lipid biomarkers for *E. huxleyi* calcification state, ploidy level, and an overall ungrazed state	Strain-specific and overall lipid biomarkers for grazed *E. huxleyi*	Strain-specific and overall lipid biomarkers for *O. marina* fed each of the four *E. huxleyi* strains

METHODS

AIM Ia: Naked vs. Calcified *E. huxleyi*

For this and subsequent analyses, I performed numerous principal component analyses (PCA) and partial least squares-discriminant analysis (PLS-DA) using lipidomic data for *E. huxleyi* or *O. marina* specific to the comparison being performed (Table 2). For AIM I analyses, the lipidomes for all four *E. huxleyi* strains in the control (ungrazed) state were used. PLS-DAs were used for analysis only when the corresponding PCA plot(s) did not show a clear separation between the treatments being compared. A PCA is an unsupervised method which clusters samples based on similarity. A PLS-DA is a supervised method which compares variables depending on how the data are classified and ignores other factors which could be causing variation between the treatments. All multivariate statistics described in this thesis (PCA, PLS-DA, and oPLS-DA) were performed in MetaboAnalyst, a free web-based program designed to analyze metabolomics data sets. Results obtained from MetaboAnalyst (loadings, weightings, fold changes, etc.) were explored in Microsoft Excel.

For the naked vs. calcified data upload onto MetaboAnalyst (see supplementary material part I for step-by-step instructions), I grouped the two naked strains together (374 and 379) and the two calcified strains together (607 and 624) and created a PCA and PLS-DA for the comparison. The PCA (Fig. 1A) did not show relevant separation on the PC1 or PC2 axis, so the PLS-DA (Fig. 1B) was used for analysis where separation was observed between the calcified and naked strains. I began my analysis by analyzing lipids with the lowest and highest 30 weights from the component 1 axis, which separated the strains based on calcification state. From MetaboAnalyst, I downloaded the PLS-DA weights, fold change in relative concentration, T-Tests and P-values for each lipid. The T-Test results were from the comparison of lipid

abundance in naked vs. calcified samples. The results of all statistical tests are available upon request. In Microsoft Excel, I sorted the component 1 weights from lowest to highest, then continued work on the top 30 largest and 30 smallest loadings. With 276 total lipids, 30 lipids correspond to approximately 10% of an *E. huxleyi* lipid dataset. In Figure 1B, the PLS-DA weights with positive values correspond to lipids that are more indicative of a naked state and the weights with negative values correspond to lipids that are more indicative of a calcified state. All of the lipids used for this and subsequent analyses had significant p-values (below 0.05) for their corresponding fold changes. I then matched the lipid ID numbers, compound names obtained from the LOBSTAHS database, and lipid classes to their corresponding PLS-DA weights.

Once these steps were complete, I had an Excel spreadsheet with the 30 highest and 30 lowest PLS-DA weights, complete with the lipid identity, the class of that lipid, its fold change, and T-Test results. I summarized the lipid class composition of these high and low PLS-DA weights by making a pie graph for the 30 lipids associated with a naked state (Fig. 1C) and the 30 lipids most associated with a calcified state (Fig. 1D). Presence/absence analyses used to determine individual lipids indicative of a state or treatment were found using Venny 2.1.

AIM Ib: Haploid vs. Diploid *E. huxleyi*

To determine the impacts of ploidy level on the lipidome, a PCA was performed as described above which compared haploid strain 379 with the other three diploid *E. huxleyi* strains (374, 607, and 624). The 30 highest and 30 lowest loadings were used to identify trends in lipid classes as well as individual lipids that may serve as possible biomarkers for ploidy level in *E. huxleyi*.

AIM Ic: Commonalities among *E. huxleyi* strains

In order to identify the lipids that remain mostly constant among all four *E. huxleyi* strains, I used loadings from the naked vs. calcified PCA plot (Fig. 1A) and analyzed the PC1 loadings that were close to zero. A PCA loading which is close to zero indicates a lipid that does not change in abundance between different treatments and therefore is not indicative of any specific treatment or state but is present in all samples similarly. Using the sorted PC1 values, I located the point where negative PC1 loadings and positive PC1 loadings met and analyzed approximately 5% of the lipids above and below this score, for a total of 30 lipids.

AIM II: Impact of grazing stress on *E. huxleyi* lipidomes

In order to explore the strain-specific differences in the lipidome, a PCA was performed on each of the four individual *E. huxleyi* strains, comparing the control ("ungrazed") state to the grazer exposed ("grazed") state in each strain. To explore the overall response of *E. huxleyi* to grazing pressure regardless of strain identity, an orthogonal PLS-DA (oPLS-DA) was performed comparing all four strains in an ungrazed state to all four strains in a grazed state. oPLS-DA is a supervised method which is more accurately able to separate the variables in a dataset based on group labels (in this case, ungrazed vs. grazed) than regular PLS-DA, which takes into account more variables that are not related to group labels.

AIM III: Impact of feeding on *O. marina* lipid composition

To explore the differences in the *Oxyrrhis marina* lipidome before and after grazing on each individual *Emiliania huxleyi* strain, four PCAs were performed which compared a single *O. marina* control lipidome to *O. marina* lipidomes collected after grazing. These PCAs are available in the supplementary materials in figures S2A-D. While the PCAs did show some

separation between the unfed and fed states for *O. marina* before and after grazing, there was overlap among the 95% confidence intervals on all the plots along the PC1 axis. This seemed to be due to one of the *O. marina* control replicates (Oxy_12) not grouping tightly with the other two replicates along either the PC1 or PC2 axis. Perhaps something occurred during the cultivation or collection of this replicate which caused its lipidome to vary in numerous ways from the other two replicates. In any case, this control replicate also caused four unfed vs. fed PLS-DA plots (not shown) created for *O. marina* to be skewed. While these plots showed better separation along the component 1 axis than the PCAs showed along the PC1 axis, the highest weights (corresponding to most prominent unfed lipids) were dominated by lipids present in the errant *O. marina* replicate. For this reason, orthogonal PLS-DA plots were used for the comparison of the unfed *O. marina* lipidome vs. the *O. marina* lipidome after consuming each of the four *E. huxleyi* strains (Fig. 6A-D). The same methods described in part I of the supplementary materials document were used in MetaboAnalyst to obtain the oPLS-DAs and to analyze the 30 highest and 30 lowest scores for *O. marina* after consuming each strain of *E. huxleyi*.

RESULTS

AIM Ia: Naked vs. Calcified

The PCA analysis comparing naked strains to calcified strains did not show separation between these two states along either the PC1 or PC2 axes (Fig. 1A). The PC1 axis seemed to be separating based on ploidy level, with lipids more indicative of diploid strains 374, 607, and 624 assigned negative loadings, and lipids more indicative of haploid strain 379 being assigned positive loadings. The PC2 axis did not separate based on any comparison I am performing in

this thesis. Because the PCA indicated that the control lipidomes of the four *E. huxleyi* strains have their strongest differences based on ploidy level, a PLS-DA was used to compare the lipidomes of the naked and calcified strains (Fig. 1B). This analysis demonstrated clear separation between the lipidomes of the naked strains and those of the calcified strains, which accounted for >36% of the variation in the lipidomes. The PLS-DA weights with positive values correspond to lipids that are more indicative of a naked state and the weights with negative values correspond to lipids that are more indicative of a calcified state. The second component shows the variation between the two strains in each grouping, indicating that the two calcified lipidomes have more in common with one another than the two naked lipidomes have in common with each other.

An analysis of the lipids with the largest weights on component 1 of the PLS-DA for naked vs. calcified strains revealed trends in lipid class and individual lipids of note for each state (Figs. 1C and 1D). Specifically, PCs, Fuco lipids, cholesterol esters, coprostanol esters, MGDGs, DAGs, BLLs, PGs, and PDPTs were representative of calcified strains, while DGDGs, S_DGCCs, BLLs, PGs, and TAGs were more characteristic of naked strains.

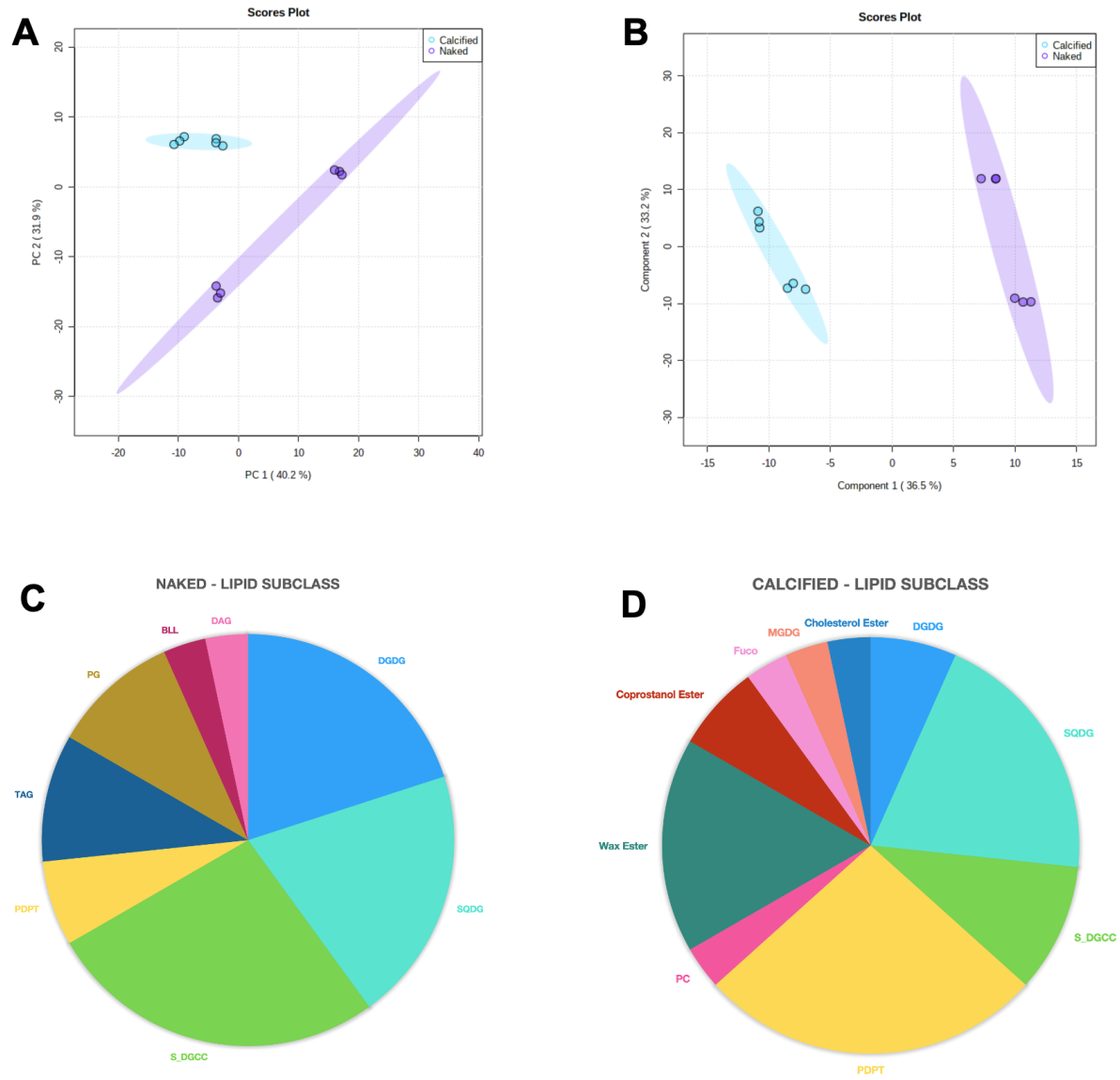

Figure 1. Results of the naked vs. calcified analysis of the *Emiliania huxleyi* lipidome. **A**, PCA scores plot of naked strain lipidomes (374, 379) vs. calcified strain lipidomes (607, 624). **B**, PLS-DA scores plot of naked strain lipidomes (374, 379) vs. calcified strain lipidomes (607, 624). Lipids with negative weights on the first component in the PLS-DA correspond to lipids more prevalent in calcified strains (blue), while lipids with positive weights correspond to lipids more prevalent in naked strains (purple). **C**, Pie graph representing a breakdown of the 30 most prominent lipid classes in naked strains, identified via the largest positive component 1 loadings from the PLS-DA. **D**, Pie graph representing a breakdown of the 30 most prominent lipid classes in calcified strains, identified via the largest negative component 1 loadings from the PLS-DA.

While the PLS-DA identified lipids whose changes in abundance are strongly indicative of a certain state, it was important to examine presence/absence data as well. Through examining the entire *E. huxleyi* lipids dataset, I uncovered which lipids are only present in certain strains.

When looking at lipids unique to naked strains, six lipids were present in strains 374 and 379 only (PDPT 32:2 +2O, PG 46:0 +4O, S_DGCC 46:3 +1O, S_DGCC 37:5 +4O, BLL 49:4 +1O, and TAG 62:15 +3O). Notably, five of these lipids were also relevant in the PLS-DA (Table 3).

Table 3. A list of lipids that are present only in naked *Emiliania huxleyi* strains that are also present in the top 30 naked PLS-DA weights. The lipid name ("Lipid"), the lipid's rank (1-30) in the PLS-DA weights ("PLS-DA Rank"), and the P-value from a t-test of peak areas in naked vs. calcified strains ("P-value") are provided.

Lipid	PLS-DA Rank	P-value
S_DGCC 37:5 +4O	5	1.71 x 10-6
PG 46:O +4O	9	3.71 x 10-5
S_DGCC 46:3 +1O	10	3.15 x 10-5
PDPT 32:2 +2O	11	8.43 x 10-6
BLL 49:4 +1O	16	1.46 x 10-4

Five lipids were unique to calcified strains 607 and 624 (MGDG 37:1 +3O, S_DGCC 43:1 +4O, PC 40:10, PDPT 36:1 +4O, PDPT 41:2 +2O). All five of these lipids were also found to be listed prominently on the sorted PLS-DA loadings for a calcified state (Table 4). These lipids are possible biomarkers for calcification in *E. huxleyi*.

Table 4. A list of lipids that are present only in calcified *Emiliania huxleyi* strains that are also present in the top 30 calcified PLS-DA weights. The lipid name ("Lipid"), the lipid's rank (1-30) in the PLS-DA weights ("PLS-DA Rank"), and the P-value from a t-test of peak areas in naked vs. calcified strains ("P-value") are provided.

Lipid	PLS-DA Rank	P-value
PDPT 41:2 + 2O	1	3.4 x 10-7
S-DGCC 43:1 +4O	2	4.25 x 10-7
MGDG 37:1 +3O	3	7.02 x 10-7
PDPT 36:1 +4O	4	1.08 x 10-6
PC 40:10	9	1.53 x 10-5

AIM Ib: Haploid vs. Diploid

The PCA which compared the lipidomes of the haploid vs. diploid strains revealed separation along the PC1 axis (Fig. 2A) which explains >40% of the variation among lipidomes. The scores with positive values correspond to haploid strain 379, while the scores with negative values correspond to lipids from diploid strains 374, 607, and 624.

An analysis of PCA loadings for the haploid vs. diploid strains revealed trends in lipid class between these two states (Fig. 2B and C). When compared to the diploid strains, the top loadings for haploid strain 379 contained a higher percentage of SQDGs and S-DGCCs. Conversely, the top loadings for the diploid strains contained coprostanol esters, cholesterol esters, and cholesterol acetate, along with a higher proportion of wax esters than the haploid strain.

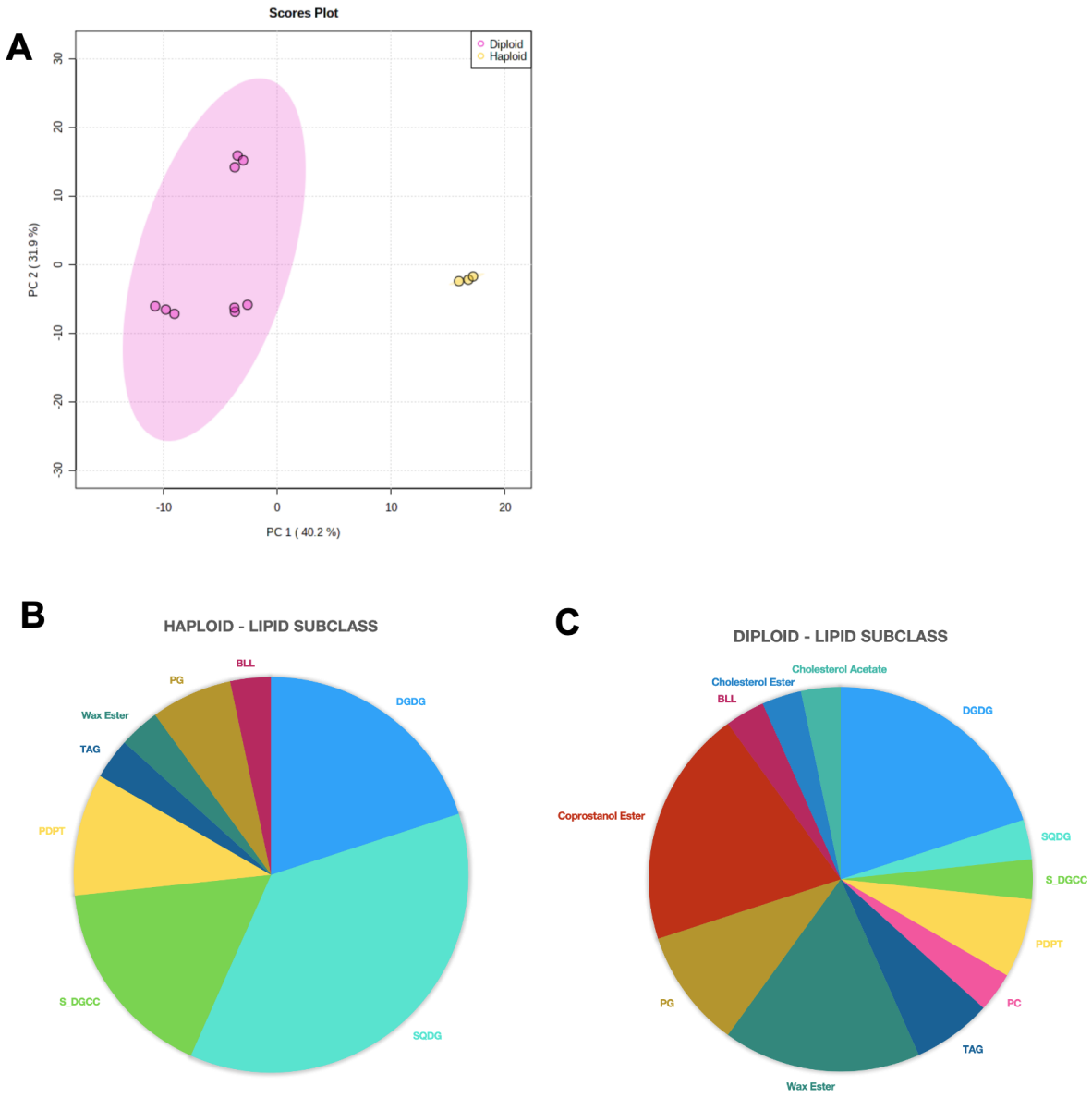

Figure 2. Results of the haploid vs. diploid analysis of the *Emiliania huxleyi* lipidome. **A**, PCA scores plot of haploid strain lipidome 379 (yellow) vs. diploid strain (374, 607, 624) lipidomes (pink). The majority of the variation between the haploid and diploid lipids is explained by PC1 (40.2%). **B**, Classes of the 30 lipids with the largest PC1 loadings, indicative of haploid strain 379. **C**, Classes of the 30 lipids with the smallest PC1 loadings, indicative of diploid strains.

Three lipids were present only in haploid strain 379 (TAG 64:16, TAG 59:13, S_DGCC 50:4 +1O) (Fig. 3), yet none of these three lipids were present in the lipids with the largest 30 PC1 loadings. The three lipids found by the PCA to be the most indicative of a haploid state were PDPT 34:4 +1O, PDPT 28:0, and DGDG 32:3. Twenty-two lipids were shared by diploid

strains 374, 607, and 624. Of these 22 lipids, there were four cholesterol esters, three coprostanol esters, three DGDGs, two wax esters, two TAGs, two S_DGCCs, two PGs, one BLL, one PC, one PDM, and one SQDG. Nineteen of these lipids were present in the top 30 diploid loadings of the PCA (Table 5).

Table 5. A list of lipids that are present only in diploid *Emiliania huxleyi* strains that are also present in the top 30 diploid PCA loadings. The lipid name ("Lipid"), the lipid's rank (1-30) in the PCA loadings ("PCA Rank"), and the P-value from a t-test of peak areas in haploid vs. diploid strains ("P-value") are provided.

Lipid	PCA Rank	P-value
Coprostanol Esters 25:2 +2O	1	4.99 x 10-11
Coprostanol Esters 25:1 +2O	2	6.97 x 10-11
Cholesterol Esters 24:1 +2O	3	1.24 x 10-10
BLL 40:10 +4O	4	5.21 x 10-8
S-DGCC 38:0 +3O	5	1.69 x 10-10
DGDG 35:5 +2O	6	1.75 x 10-10
DGDG 35:6 +2O	7	1.25 X 10-9
Coprostanol Esters 24:2 +3O	8	1.86 x 10-8
Cholesterol Esters 25:1 +3O	9	2.29 x 10-9
PG 40:1 +4O	11	1.32 x 10-9
Wax Ester 32:2 +1O	15	3.47 x 10-6
TAG 62:16 +2O	16	2.89 x 10-6
SQDG 30:1	17	1.53 x 10-6
PG 47:0 +4O	19	1.22 x 10-5
Cholesterol Esters 25:2 +3O	22	1.87 x 10-5
DGDG 37:6	23	3.62 x 10-5
TAG 52:10	24	4.68 x 10-6
Coprostanol Esters 11:0	26	5.15 x 10-5
PC 38:9 +1O	29	7.83 x 10-5

AIM Ic: Shared *E. huxleyi* Lipids

To find lipids that are common across all four strains of *E. huxleyi* tested, the 30 lipids with loadings closest to zero for the PCA used in aim I (Fig. 1A) revealed lipids that are consistently present in all four strains tested. A breakdown of these loadings revealed many of the same lipid classes as the earlier analyses. DGDGs, SQDGs, S_DGCCs, and TAGs were all prominent. One lipid class that was revealed only in this comparison, however, was PUA, a type of oxylipin that is formed by fatty acids when phytoplankton are stressed (Ribalet et al., 2014).

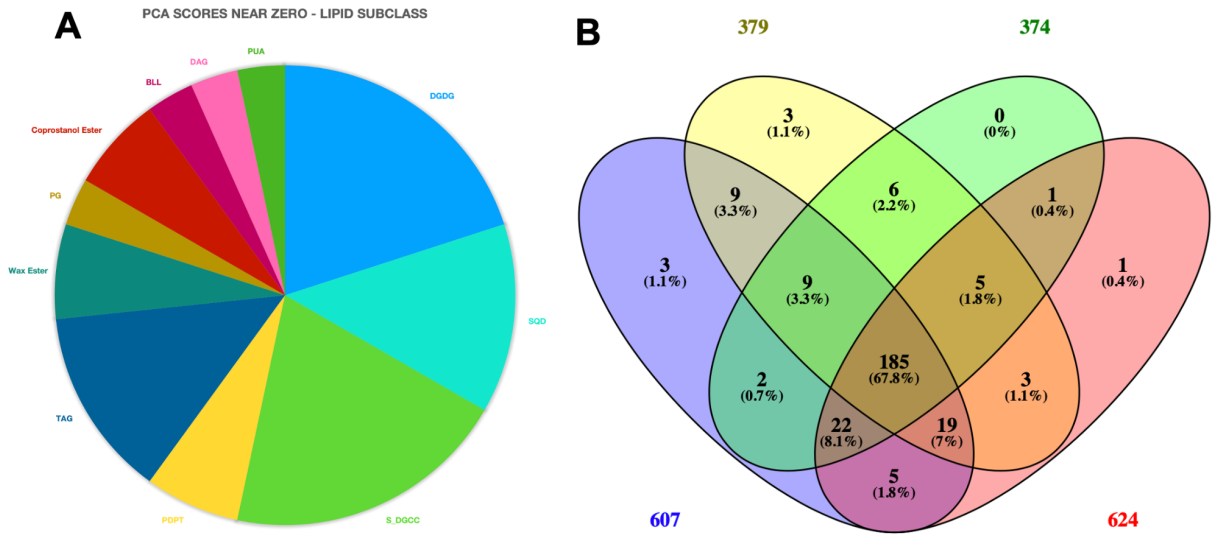

Figure 3. *Emiliania huxleyi* lipids that are present in similar amounts in all four strains, regardless of ploidy level or calcification state. **A**, Lipid classes represented in the 30 loadings closest to zero on PC1. **B**, Venn diagram comparing the lipidomes of all four *E. huxleyi* strains (created using Venny 2.1).

My analysis revealed that out of 276 total *E. huxleyi* lipids, 185 lipids (>67%) were shared by all four ungrazed strains (Fig. 3B). Of these 185 lipids, 22 had PC1 loadings near zero (Table 6), showing that there is consistency in the lipid profiles of different strains.

Table 6. A list of lipids that are present in all four ungrazed *Emiliania huxleyi* strains which also have PC1 loadings near zero. The lipid name, ("Lipid") and the PC1 loading value ("PC1 Loading") are provided.

Lipid	PC1 Loading
SQDG 32:1	-0.017896

DGDG 36:9	-0.013979
Wax Ester 41:4 +2O	-0.012256
S_DGCC 28:3 +1O	-0.011397
DGDG 21:2 +2O	-0.010109
SQDG 33:3	-0.007791
S_DGCC 35:4	-0.006791
PDPT 37:6	-0.005667
PUA 12:2	-0.003361
DAG 36:9	-0.001143
SQDG 40:8	0.0034094
SQDG 29:0	0.0037516
PDPT 38:3 +4O	0.0042128
DGDG 34:6	0.0043485
DGDG 36:10	0.0045905
S_DGCC 36:9 +3O	0.0048069
Coprostanol Esters 18:2 +4O	0.0079783
TAG 56:2	0.009371
S_DGCC 43:8 +4O	0.011026
S_DGCC 39:8 4O	0.011042
S_DGCC 28:0 +2O	0.012071
TAG 52:9	0.012682

AIM IIa: Individual strain responses to grazing stress

The *E. huxleyi* lipidome showed marked differences between an ungrazed and a grazed state, both within individual strains (Fig. 4) and when comparing all four strains (Fig. 5). When looking at strain specific responses, PCA showed clear separation between ungrazed and grazed-stressed conditions along PC1 (Fig. 4A-D). In each PCA, the loadings with negative values correspond to lipids in an ungrazed (control) state, while the loadings with positive values correspond to lipids in a grazed state.

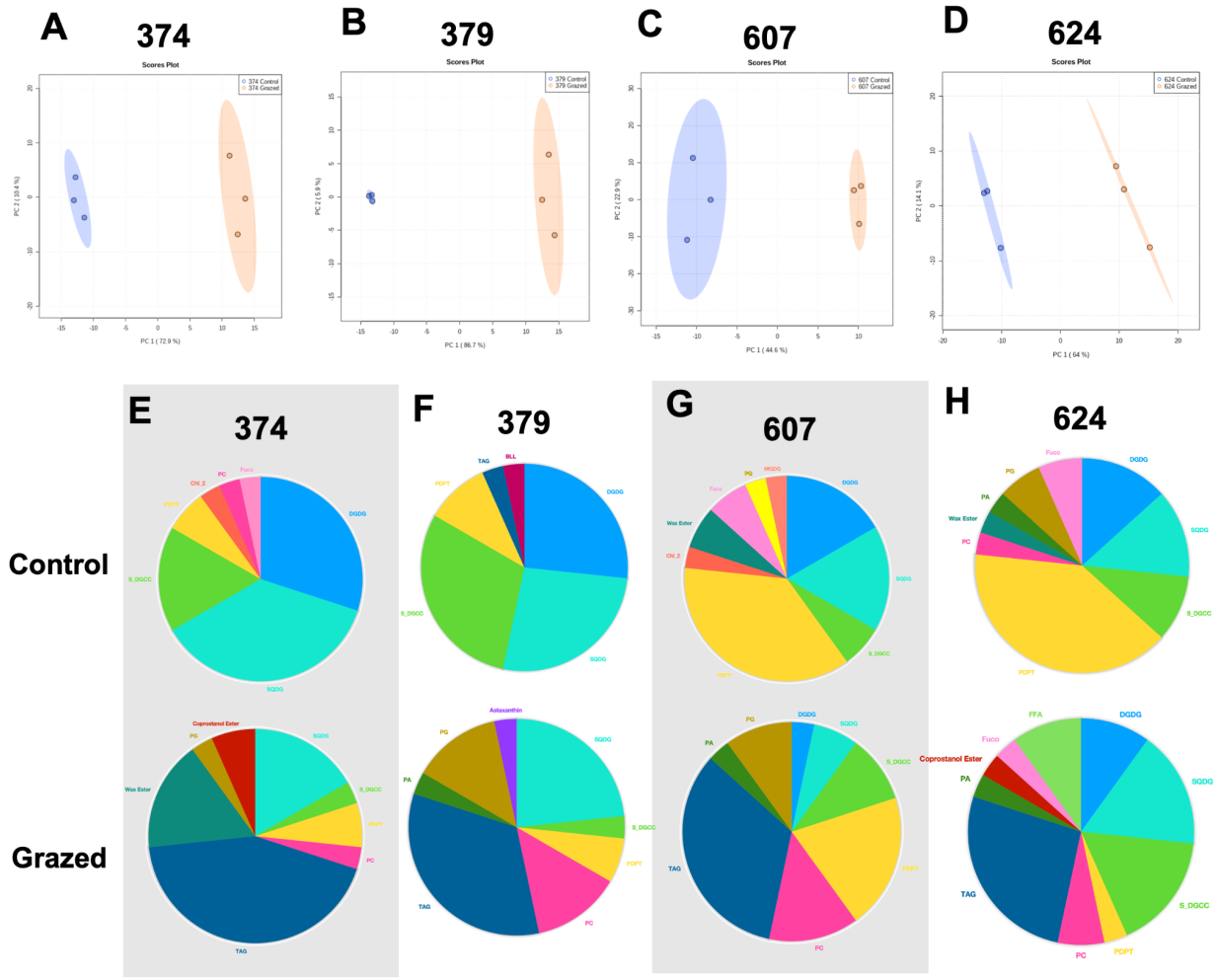

Figure 4. Results of the ungrazed vs. grazed lipidome analysis of all four individual *Emiliania huxleyi* strains. PCA scores plot of **A**, strain 374 lipidome **B**, 379 lipidome **C**, 607 lipidome and **D**, 624 lipidome. The negative PC1 scores on each plot correspond to lipids in an ungrazed state (blue), while the positive scores on each plot correspond to lipids in a grazed state (tan). **E**, Lipid classes represented in the 30 lipids with lowest loadings on PC1 in ungrazed strain 374 ("Control") and the 30 lipids with the highest loadings ("Grazed"). **F**, Lipid classes represented in the 30 lipids with lowest loadings on PC1 in ungrazed strain 379 ("Control") and the 30 lipids with the highest loadings ("Grazed"). **G**, Lipid classes represented in the 30 lipids with lowest loadings on PC1 in ungrazed strain 607 ("Control") and the 30 lipids with the highest loadings ("Grazed"). **H**, Lipid classes represented in the 30 lipids with lowest loadings on PC1 in ungrazed strain 624 ("Control") and the 30 lipids with the highest loadings ("Grazed").

Analyses of the top 30 PCA loadings for ungrazed and grazed states in each individual *E. huxleyi* strain revealed similarities and differences in the classes of lipid that were indicative of exposure to grazers. These lipid class breakdowns are visible in figures 4E-H. In all four strains, a grazed state was strongly associated with the presence of TAGs, which made up between 30 - 45% of the lipids present in the top 30 loadings associated with grazed state for each strain.

Grazing was also associated with a decrease in DGDGs and an increase in PC lipids in all four strains.

There were also many differences in the lipid class breakdowns that were limited to specific strains. In strain 374 (Fig. 4E) prominent "grazed" lipids were unique in that they contained a large percentage of wax esters. Lipids with large loadings in strain 379 (Fig. 4F) were unique in that they contained astaxanthin, a pigment lipid with a myriad of uses ranging from a purported human health supplement to pigmentation for animal products (Ambati et al., 2014). The top loadings for strain 624 (Fig. 4H) were unique in that they contained FFAs.

There were also many differences in lipid class breakdowns that were associated with various subsets of *E. huxleyi* strains. For instance, the lipids with high loadings in strains 374 and 624 contained coprostanol esters, and the top loadings for strains 374, 379, and 607 contained PGs, suggesting that the relative concentrations of these lipids were increased in grazer-exposed cultures. Interestingly, the lipids with large loadings in calcified strains 607 and 624 contain DGDGs, while the naked strains do not appear to have DGDGs as biomarkers for grazing.

AIM IIb: Common responses to grazing stress

While each individual *E. huxleyi* strain showed numerous unique differences between ungrazed and grazed states, the comparison of the ungrazed vs. grazed states of all four combined strains revealed the lipid classes that are indicative of a generalized grazer exposed state. Due to considerable variation in how the lipidomes of each strain changed in response to grazing, neither the PCA (Fig. 5A) nor the PLS-DA (Fig. 5B) performed on the combined *E. huxleyi* lipidomes showed separation between the control and grazed states on either axis. In order to properly analyze the lipids most indicative of ungrazed and grazed states, an orthogonal PLS-DA (oPLS-DA) was performed (Fig. 5C). The oPLS-DA separated the lipids according to

their ungrazed and grazed states, with this variation being accounted for by the T score on the first axis. In the oPLS-DA, lipids that are more prevalent in an ungrazed state have negative loadings whereas lipids with positive loadings are indicative of exposure to grazers.

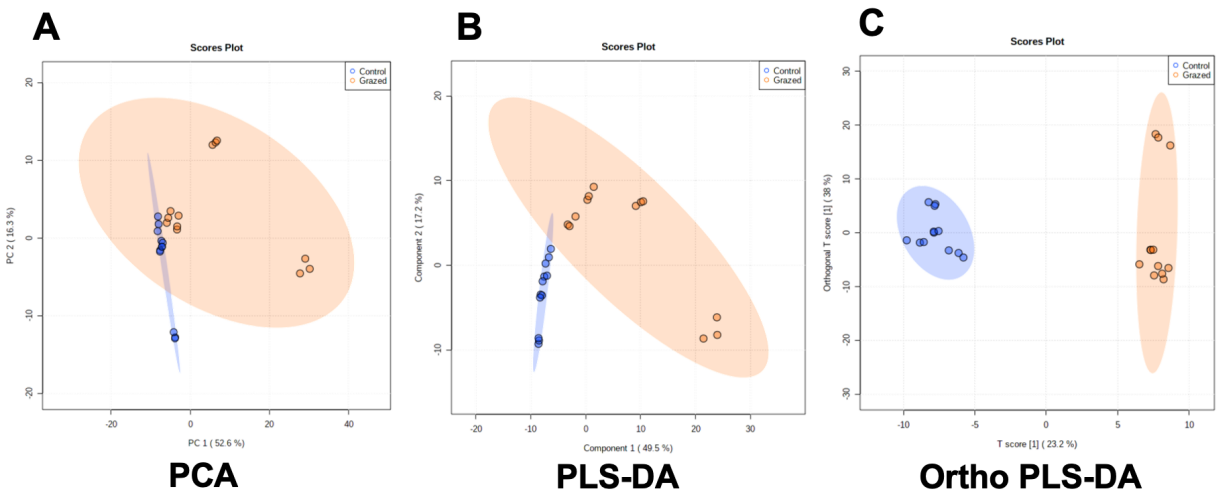

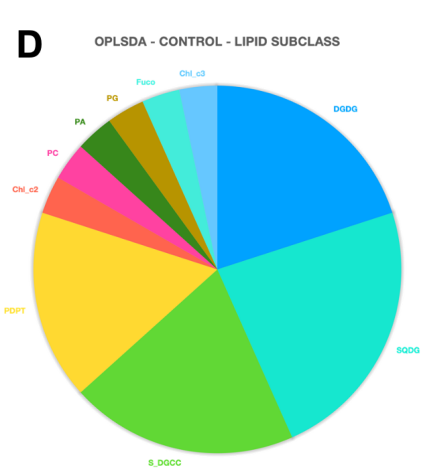

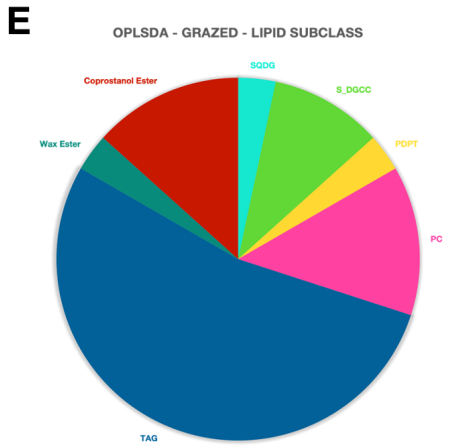

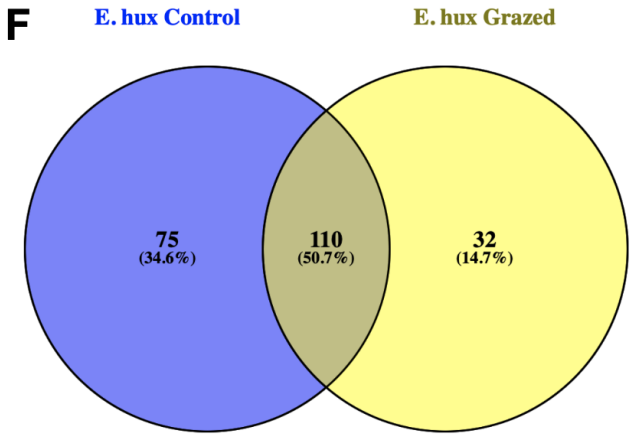

Figure 5. Results of the ungrazed vs. grazed lipidome analysis of all four *Emiliania huxleyi* strains. **A**, PCA scores plot comparing all four *E. huxleyi* strains in ungrazed cultures ("control") and grazer exposed ("grazed") cultures. **B**, PLS-DA plot comparing all four *E. huxleyi* strains in an ungrazed state to all four strains in a grazed state. **C**, Orthogonal PLS-DA comparing all four *E. huxleyi* strains in an ungrazed state to all four strains in a grazed state. In all three plots, the negative scores/loadings along the PC1/component 1/T score axes correspond to lipids in an ungrazed state (blue), while the positive scores on each plot correspond to lipids in a grazed state (tan). **D**, Control lipid classes represented in the 30 lipids with the lowest scores on T score 1. **E**, Grazed lipid classes represented in the 30 lipids with the highest scores on T score 1. **F**, Venn diagram comparing the 185 lipids shared by all four *E. huxleyi* strains in ungrazed ("control") cultures to the 142 lipids shared by all four *E. huxleyi* strains in grazed cultures.

Analysis of the top 30 oPLS-DA loadings for ungrazed and grazed cultures for all four *E. huxleyi* strains revealed remarkable differences between the two groupings of lipids. The lipid breakdown indicates that lipid classes most indicative of ungrazed cultures are SQDGs, DGDGs, S_DGCCs, and PDPTs (Fig. 5D). Lipid classes most indicative of a grazed state in *E. huxleyi* are TAGs, coprostanol esters, PCs, and wax esters (Fig 5E). One very notable trend within and among strains, was the sharp reduction in DGDG lipids associated with grazed cultures.

A Venn diagram comparing the grazed lipidomes of all four *Emiliania huxleyi* strains is available in the supplementary materials (Fig. S1). This comparison revealed lipids unique to strains 374 and 607 after grazing and revealed numerous lipids that were shared by two or more strains after grazing. The single lipid unique to grazed strain 374 was wax ester 32:0 +3O. However, this lipid was not present in the top 30 grazed PCA loadings for this individual strain, nor was it present in the oPLS-DA loadings corresponding to grazing in all strains. The Venn

diagram also revealed two lipids unique to grazed strain 607 only: PC 44:10 and TAG 59:14 +1O. Neither of these lipids is present in the top 30 PCA loadings associated with a grazed state in strain 607, but PC 44:10 is identified as indicative of a grazed state in the top loadings of the combined strain oPLS-DA analysis.

While there were only three lipids unique to individual *E. huxleyi* strains in a grazed state, there were 35 lipids shared by two strains, 93 shared by three strains, and 142 total lipids being shared among all four (Fig. S1). Out of these 142 shared lipids, 32 (>14%) were unique to a grazed state (Fig. 5F). Of these 32 lipids, 19 were present in the top loadings taken from the combined-strain oPLS-DA in figure 5C and are listed in Table 7. Any or all of these lipids are potential biomarkers for a grazed state in *Emiliania huxleyi*.

Table 7. A list of lipids only present in all four grazed *Emiliania huxleyi* strains that are also present in the top 30 oPLS-DA loadings. The lipid name ("Lipid"), the lipid's rank (1-30) in the orthogonal PLS-DA weights ("oPLS-DA Rank"), and the P-value from a t-test of peak areas in control vs. grazed strains ("P-value") are provided.

Lipid	oPLS-DA Rank	P-value
PC 42:10 +1O	1	4.64 x 10-10
PC 44:11 +3O	2	7.43 x 10-9
Coprostanol Esters 24:2 +4O	3	2.16 x 10-7
TAG 64:15 +3O	4	1.08 x 10-6
TAG 53:8	5	7.13 x 10-7
TAG 51:8	6	1.02 x 10-6
TAG 55:11	7	6.02 x 10-7
Coprostanol Esters 20:0 +4O	8	3.01 x 10-5
S_DGCC 48:4 +1O	9	1.28 x 10-6
TAG 53:5	11	2.27 x 10-5
TAG 55:10	17	7.13 X 10-6
Coprostanol Esters 22:1 +4O	18	8.97 x 10-5

PC 40:10	20	4.39 x 10-5
Coprostanol Esters 24:1 +4O	23	5.20 x 10-4
PC 42:10 +1O	24	4.32 x 10-4
TAG 62:15 +3O	26	1.90 x 10-4
S_DGCC 46:3 +1O	27	1.46 x 10-4
TAG 52:10	29	3.64 x 10-4
S_DGCC 50:4 +1O	30	7.00 x 10-4

AIM III: *O. marina* lipidomic response to food

There were numerous differences in the *O. marina* lipidome after feeding on the four *E. huxleyi* strains, with only a few changes to the *O. marina* lipidome being dependent on specific strains. Overall, there appeared to be a great amount of similarity amongst the fed *O. marina* lipidomes. In the oPLS-DA plots, loadings with negative values correspond to *O. marina* lipids after grazing on one of the four *E. huxleyi* strains, and loadings with positive values correspond to *O. marina* lipids in an unfed state.

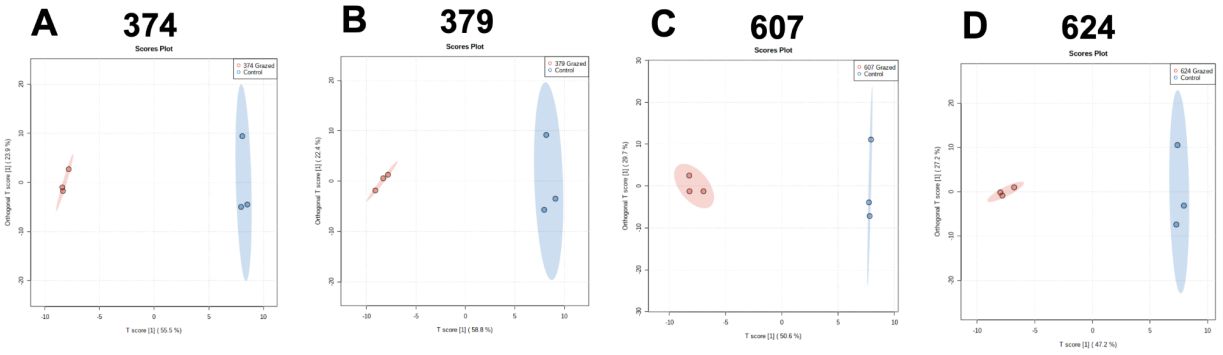

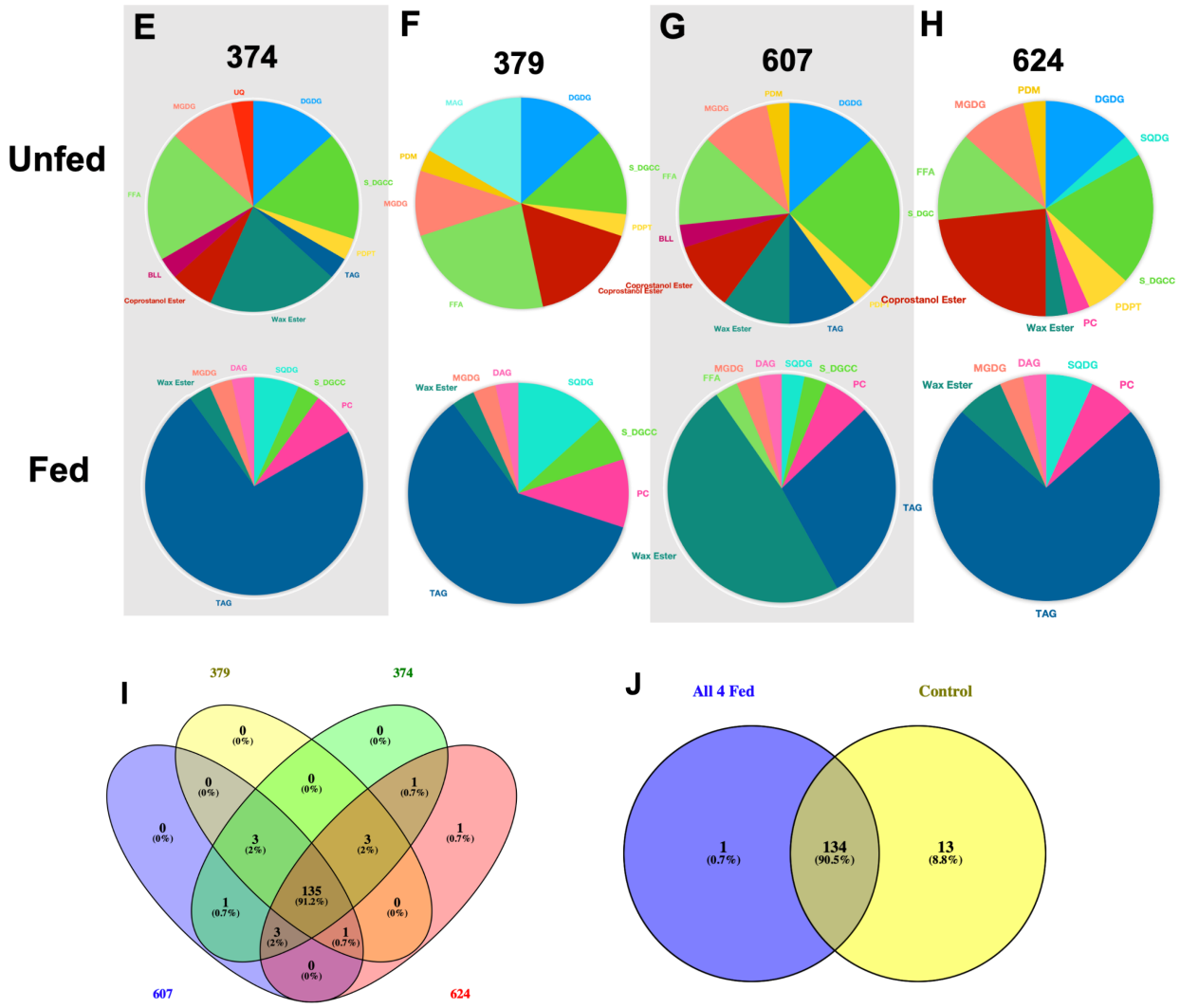

Figure 6. Results of the unfed vs. fed lipidome analysis of *Oxyrrhis marina* fed each of the four *Emiliania huxleyi* strains. Orthogonal PLS-DA scores plot of the *O. marina* lipidome before and after grazing on **A**, *E. huxleyi* strain 374. **B**, *E. huxleyi* strain 379. **C**, *E. huxleyi* strain 607. **D**, *E. huxleyi* strain 624. The negative scores on each plot correspond to *O. marina* lipids present after grazing on a specified *E. huxleyi* strain (red), while the positive scores on each plot correspond to *O. marina* lipids in an unfed state (blue). **E**, Lipid classes represented in the 30 lipids with lowest weights on T score 1 in unfed *O. marina* ("Unfed") and the 30 lipids with the highest loadings in *O. marina* fed strain 374 ("Fed"). **F**, Lipid classes represented in the 30 lipids with lowest weights on T score 1 in unfed *O. marina* ("Unfed") and the 30 lipids with the highest loadings in *O. marina* fed strain 379 ("Fed"). **G**, Lipid classes represented in the 30 lipids with lowest weights on T score 1 in unfed *O. marina* ("Unfed") and the 30 lipids with the highest loadings in *O. marina* fed strain 607 ("Fed"). **H**, Lipid classes represented in the 30 lipids with lowest weights on T score 1 in unfed *O. marina* ("Unfed") and the 30 lipids with the highest loadings in *O. marina* fed strain 624 ("Fed"). **I**, Venn diagram of the *O. marina* lipidome after being fed each of the four *E. huxleyi* strains. **J**, Venn diagram comparing the lipids shared by all four *O. marina* fed lipidomes to the *O. marina* control (unfed) lipidome.

A breakdown of the lipid classes indicative of unfed and fed states in *O. marina* after consumption of each of the four *E. huxleyi* strains reveals several interesting trends in lipid class

(Fig. 6E-H). Overall, the lipid class most indicative of a fed state in *O. marina* was TAGs, with this lipid class making up between 25% - 75% of the top oPLS-DA fed loadings. Another lipid class found to be more prominent in a fed state than an unfed state regardless of food sources was PCs as well as one DAG lipid (DAG 44:12). Overall, the prominent lipid classes in *O. marina* fed *E. huxleyi* strains 374, 379, and 624 were largely similar. However, the lipidome of *O. marina* consuming *E. huxleyi* strain 607 (Fig. 6G fed) had a striking difference; nearly 50% of the top oPLS-DA loadings were wax esters: *O. marina* fed strain 607 had 14 wax esters in the top 30 oPLS-DA loadings, while the *O. marina* fed the other three strains had only one or two wax esters prevalent in their lipidomes.

There were numerous lipids which were unique to *O. marina* having grazed on one or more *E. huxleyi* strains (Fig. 6I). One lipid, S_DGCC 31:3 +1O was present in the *O. marina* lipidome only after feeding on strain 624, however it was not present in the oPLS-DA loadings for a fed state after consuming strain 624. The presence of this lipid in the control *O. marina* lipidome means that this is not a potential biomarker for *O. marina* after feeding on strain 624.

Three lipids, wax ester 27:4 +2O, wax ester 49:2 +1O, and DAG 33:0 +4O were present in *O. marina* only after consuming strains 374, 607, and 624. However, all three of these lipids were present in the *O. marina* unfed lipidome as well, and none of these three lipids were present in the top 30 fed oPLS-DA loadings for *O. marina* after grazing on each of these three *E. huxleyi* strains. Therefore, these three lipids are not appropriate biomarker lipids indicative of *O. marina* consuming diploid *E. huxleyi*.

A comparison of the 135 lipids present in *O. marina* after being fed each of the four *E. huxleyi* strains to the *O. marina* control lipidome is shown in figure 6J. 134 lipids are present in *O. marina* in both a control state and after feeding on all four *E. huxleyi* strains. One lipid, PC

44:12 +4O, is present in *O. marina* only in a fed state. This lipid was found among the top 30 fed oPLS-DA loadings only in the strain 607 analysis (with a loadings rank of 22). The presence of this lipid in the fed state only after feeding on all four *E. huxleyi* strains and its prominence in one of the oPLS-DAs makes this lipid a potential biomarker of a fed state in *O. marina*, at least within the scope of the dataset used for this report.

The lack of individual lipid biomarkers for *O. marina* fed specific *E. huxleyi* strains was striking. Only one lipid, S_DGCC 31:3 +1O, was unique to the *O. marina* lipidome after consuming *E. huxleyi* strain 624, and three lipids were unique to *O. marina* after consuming diploid strains of *E. huxleyi* (374, 607, and 624). However, all four of these lipids were also present in the unfed *O. marina* lipidome, and none were found to be prominent in the top 30 oPLS-DA loadings for *O. marina* fed these respective strains. Contrary to this, of the 148 total *O. marina* lipids present after grazing, 135 were shared by *O. marina* after feeding on each of the four *E. huxleyi strains*. This illustrates that the vast majority of *O. marina* lipids were upregulated in response to grazing regardless of which *E. huxleyi* strain was consumed. Some lipids were more upregulated after consuming some strains when compared to others, for instance, the predominance of wax esters in *O. marina* after consuming *E. huxleyi* strain 607, but the individual lipids created were by and large, shared. This makes sense, as within a given species, many of the same lipids are created despite varied sources of food, as the same biosynthetic pathways are at play when digesting each of the four *E. huxleyi* strains (Dairi et al., 2011).

DISCUSSION

AIM Ia: *E. huxleyi* lipidomes differ based on calcification state

My comparison of naked (strains 374 and 379) and calcified (strains 607 and 624) revealed differences in lipid class composition in naked vs. calcified strains. Coccoliths are intricate calcium carbonate sheets which form in layers around cells in calcified strains of *E. huxleyi* and have multiple functions. In my analysis, the presence of wax esters and coprostanol esters in the largest PLS-DA loadings indicates that these lipid classes could be important predictors of calcification in *E. huxleyi*. There are many published works that study these lipid classes in zooplankton (where they serve as long-term storage lipids), but few investigate the functioning of these lipids in phytoplankton. In the plant *Arabidopsis thaliana*, wax esters on the surface of leaves and stems are associated with tolerance to drought (Patwari et al., 2019), and are also important components on the surfaces of primary shoots and within seed oils (Li et al., 2008). Coprostanol esters are a product of cholesterol metabolism, and in plants, coprostanol esters accumulate in seeds and cell membranes. In seeds, they help with cell proliferation and differentiation, and in cell membranes they can help regulate fluidity and permeability (Piironen et al., 2000). Naked and calcified strains have many differences in their biochemical pathways and internal structures (Taylor et al., 2017), and the observed differences in my analysis could reflect this. Calcite coccoliths are created within the cell, inside of specialized compartments called coccolith vesicles. Once mature, coccoliths are moved to the membrane exterior where they assemble in layers to surround the cell (Brownlee et al., 2015). One possibility then for the observed differences in lipid class makeup, is that the lipid classes found to be more prominent in calcified *E. huxleyi* are components of these coccolith vesicles or are otherwise involved in the myriad of biosynthetic processes required to create coccoliths.

Another possibility is that calcified coccolithophores inhabit different environmental niches and experience a different suite of stressors than their naked counterparts, leading to differences in lipid makeup that provide advantages to these habitats. For instance, it has been suggested that calcified *E. huxleyi* are typically found deeper in the water column than naked cells (Taylor et al., 2017), which provides a possible explanation for the greater quantity of coprostanol esters observed in the calcified PLS-DA weights. Deeper water is usually cooler than surface water, so cholesterol and corresponding coprostanol esters in the membranes of *E. huxleyi* could help maintain membrane fluidity at these greater depths. Wax esters help provide structural support and protection against dehydration in *A. thaliana*, and they could provide similar advantages to calcified *E. huxleyi*. The deeper a cell is in the water column, the greater the water pressure that cell will experience. Thus, it is possible that wax esters are present in greater amounts due to their possible role in helping to maintain cell shape and integrity in calcified *E. huxleyi*.

AIM Ib: Ploidy level influences *E. huxleyi* lipid composition

My comparison of haploid strain 379 and diploid strains 374, 607, and 624 revealed differences in lipid class composition based on ploidy level. One possible explanation for these differences has to do with the different susceptibilities of haploid and diploid *E. huxleyi* to viral infection. It has been known for some time that haploid *E. huxleyi* have a natural resistance to viral infection, which diploid *E. huxleyi* do not possess. Coccolithophore populations are even able to switch from a primarily diploid to a primarily haploid composition in response to viral infection (Frada et al., 2008). *E. huxleyi* viruses (EhVs) penetrate host cells via membrane fusion and leave host cells via budding, which requires a host cell membrane that will readily fuse with a viral lipid envelope and results in viruses leaving a host while containing host-cell lipids

(Fulton et al., 2014). Haploid *E. huxleyi* could contain membrane lipids that prevent this viral fusion, while diploid *E. huxleyi* could contain membrane lipids that facilitate it. Numerous studies have found that sGSL (glycosphingolipid) content in *E. huxleyi* cell membranes is positively correlated with susceptibility to viral infection (Fulton et al., 2014). However, no prominent glycosphingolipids were found in my analysis, which suggests these lipids are not influential in grazing. Studies have also found that EhV infection leads to extreme remodeling of the host-cell lipidome (Hunter et al., 2015). It is possible that haploid *E. huxleyi* is also less susceptible to this remodeling than diploid *E. huxleyi*.

One study of viral infection in *E. huxleyi* haploid vs. diploid cells obtained data on an uninfected haploid and diploid strain (Hunter et al., 2015), which was useful to compare to my own results. Possible haploid biomarkers identified by Hunter et al. (2015) were WE 31:0, GSL 40:0 and 40:1, and MGDG 32:5, although none of these were present in the lipidome obtained for haploid *E. huxleyi* from the Harvey et al. (2015) analysis. Possible diploid biomarkers identified by Hunter et al. (2015) were MGDG 36:9, SQDG 40:8, BLL 18:1, PC 34:5, and numerous sGSLs. However, only one of these lipids, SQDG 40:8, was found in my analysis, and it was detected in all four *E. huxleyi* strains tested here. This suggests that this indeed may not be an ideal biomarker for diploid *E. huxleyi*, as my analysis found it was present in haploid strain 379.

Haploid and diploid cells have also been found to prefer different habitats, with haploid cells being more prolific in cool, nutrient poor waters and diploid cells being more well adapted to warmer nutrient-rich waters (Taylor et al., 2017). In my analysis, the PCA found SQDGs and betaine lipids (S-DGCCs) to be important indicators of a haploid state. SQDGs are present in thylakoid membranes and help in photosynthesis, and betaine lipids can replace phospholipids in

times of stress, such as phosphate limitation, nitrate limitation and low temperatures (Huang et al., 2019; Murakami et al., 2018). Perhaps, in nutrient poor waters, SQDGs help with additional photosynthesis necessary to power movement, and perhaps betaine lipids help haploid cells cope with environmental stress and a life spent in cooler waters. The PCA revealed that coprostanol esters, and wax esters are important indicators of a diploid state, which were also indicators of a calcified state. Because many diploid *E. huxleyi* strains are (to our knowledge) also calcified, the biomarkers for a calcified state could be similar to those for a diploid state.

AIM Ic: *E. huxleyi* strains share a core lipidome

The lipidomes of the four *E. huxleyi* strains showed remarkable variation in their changes in lipid makeup in response to grazing (see aim II), their effect on predator growth rate (Harvey et al., 2015), and in the quantity of different lipids that were present in each strain. However, there were still many shared lipids found in my analysis, with 68% of the lipids present in the *E. huxleyi* analysis found in all four strains. Astaxanthin, a red pigment lipid with numerous commercial uses (Ambati et al., 2014), was one of these shared lipids.

Other studies have found many of the same classes and individual lipids found in the Harvey et al. (2015) dataset and discussed in this analysis (Aveiro et al., 2020). However, there were numerous individual lipids and lipid classes identified in Aveiro et al. (2020) that were not present in my dataset (e.g., MMPE, sGSL, PI, etc.), and the authors mentioned that the individual lipids and lipid classes they identified differed from previous research as well. They postulated that strain identity and growth conditions can have large effects on the lipid makeup of *E. huxleyi*, making it difficult to compare studies. This variability also makes it difficult to study the lipidome of the *E. huxleyi* species as a whole. While an in-depth analysis of the *E. huxleyi* lipidome in general was not feasible for this thesis, the list of 185 lipids shared by all four strains,

as well as the lipids identified by the PCA as present but mostly unchanging between strains, does provide some clues as to what lipids were not strain-specific. For instance, the lipid class breakdown of the oPLS-DA results shows that many DGDGs, TAGs, SQDGs, betaine lipids, and wax esters are present in all *E. huxleyi* strains (Fig. 3A), and therefore may not be decent biomarker classes for ploidy level and calcification state. Rather, only individual lipids should be used for this purpose. For instance, the PUA 12:2 lipid (polyunsaturated aldehyde), was not identified by PCA analysis in either the ploidy or calcification state comparisons, so this lipid could be a biomarker lipid that remains unchanged in the four *E. huxleyi* strains used in this experiment.

A distinct limitation of the above analysis and those throughout this thesis, is that I am only working with data from four total *E. huxleyi* strains and one strain of *O. marina*. In addition, each of the four *E. huxleyi* strains differs greatly in their individual lipidomes, ploidy level, calcification state, and in how they are impacted by predation (Harvey et al., 2015). It is not yet known how many strains of *E. huxleyi* exist in the ocean, but the number is likely in the hundreds or thousands (Monteiro et al., 2016). *O. marina* also has large amounts of intraspecies variation, with 38 named strains and many more likely in existence (Lowe et al., 2011). With so few strains to work with and so much variability between the strains, applying my findings to *E. huxleyi* and *O. marina* at large is impossible.

AIM II: *E. huxleyi* lipidomes have both shared and unique responses to grazing stress

In aim I, the ungrazed lipidomes of *Emiliania huxleyi* were explored, looking at lipids common to a general unstressed state, as well as lipids specific to calcification state and ploidy level. In aim II, the impact of grazing on the *E. huxleyi* lipidome was explored, both among each individual strain and all four strains as a whole. It was discovered that while the lipidome of each

E. huxleyi strain responds to grazing in a unique way, there are some commonalities shared by all four. When looking at grazing-induced changes in the lipid classes represented in the PCAs/oPLS-DA, there were two notable changes that were shared among all four strains. These changes were a large decrease in DGDGs and a marked increase in TAGs. Another lipid class that was prominent in the combined strain analysis as well as two of the individual strains (374 and 624) was coprostanol esters. The decrease in DGDGs and corresponding increase in TAGs, as well as the presence of coprostanol esters and their possible connections to a grazed state will be discussed below.

One initial worry during initial analysis of aim II data, was that the TAGs present in the grazer exposed *E. huxleyi* lipidomes could be contamination from the *Oxyrrhis marina* lipidome. However, terrestrial plants as well as many types of phytoplankton not only produce small amounts of TAGs at all times but accumulate TAGs in large quantities in response to changes in their environment (Lu et al., 2020; Sayanova et al., 2017). In diatoms and other types of phytoplankton, cells can produce large amounts of TAGs in response to nutrient deprivation and other environmental stressors, such as high temperatures and light intensity (Maeda et al., 2017; Zienkiewicz et al., 2016). Most of these TAGs are created through the remodeling of lipids in the chloroplast membrane (Maeda et al., 2017). In the present study, DGDGs (present in thylakoid membranes) experienced a large decrease along with the corresponding increase in TAGs when exposed to grazers (Fig. 5D and E). If the DGDGs in *E. huxleyi* are being remodeled into TAGs in response to grazing pressure, this would explain both the increase in TAGs and the decrease in DGDGs observed in this analysis. Indeed, studies have shown that TAG formation is highly correlated with chloroplast degradation in phytoplankton, with increases in TAGs occurring in concert with decreases in chloroplast membrane and pigment lipids (Zienkiewicz et al., 2016).

The lipid classes most indicative of an ungrazed state in *E. huxleyi* include two chloroplast pigment lipids, and a large number of the chloroplast membrane lipids DGDGs and SQDGs (Fig. 5D). The lipids most indicative of a grazed state do not include DGDGs, include only one SQDG lipid, no chloroplast pigment lipids, and a large number (over half of the 30 most prominent grazed lipids) of TAGs (Fig 5E).

One possible reason for chloroplast degradation in favor of TAG production is that stressful conditions cause phytoplankton cells to enter into a quiescence phase (Zienkiewicz et al., 2016). In this phase, cells temporarily stop dividing and rewire their metabolisms in a way that will best help them survive the stressful situation. Typically, this means taking apart the photosynthetic membranes in chloroplasts and using those lipids to create massive amounts of TAGs, which provide energy to the cell throughout the stressful period. While the environmental stressors explored in the literature center around nutrient deprivation, elevated temperatures, and light stress, it is reasonable to assume that grazing pressure from a protist predator could invoke a very similar stress response in phytoplankton.

Coprostanol esters are a type of plant sterol, which are plant compounds similar in structure to cholesterol. Plant sterols play many roles, such as signal transduction and the regulation of membrane fluidity (Piepho et al., 2010). Studies have found that plant sterols increase in response to environmental stressors, such as nutrient deprivation and high light intensity (Gordillo et al., 1998; Piepho et al., 2010). The exact biochemical pathways involved in creating these plant esters are not as well studied as those involved in TAG synthesis. While the analysis of grazer exposure responses in the four *E. huxleyi* strains used in this analysis indicates coprostanol esters are prominent lipids produced in response to grazing pressure, there is not enough evidence to postulate why at this time.

Along with the lipidome changes shared by all four strains in response to grazing, there were also many changes in lipid classes that were strain specific. After grazing, strain 374 and the combined-strain analysis saw an increase in wax esters; strain 379 had astaxanthin present, and strain 624 had a large increase in FFAs.

In the literature, wax esters are typically discussed in relation to zooplankton, with common belief holding that marine phytoplankton contain only low levels of this type of lipid (Sargent et al., 1977). Indeed, there were surprisingly few studies that look at the role of this lipid class in phytoplankton. However, in *A. thaliana*, wax esters on the surface of leaves and stems are associated with an increased tolerance to drought (Patwari et al., 2019), and are also important on the surfaces of primary shoots and as components of seed oils (Li et al., 2008). Strain 374 experienced strong grazing pressure, second only to that experienced by 379. It's possible that the creation of TAGs and corresponding depletion of chloroplast and cell membrane lipids in the naked strain 374 leave the cells vulnerable to outside elements. Perhaps wax esters can accumulate in and on top of cell membranes, providing structural support and protection from the elements, including water loss to a high-salinity environment.

Alternatively, the reorganization of the cell membrane could be a direct response to chemical cues from *O. marina* predators. Indeed, previous research has shown that phytoplankton can respond quickly when they sense chemical cues from predators, with some species capable of inducing toxicity (Selander et al., 2015). So, it is possible that this increase in wax esters occurs in response to predation signals from both predators and other phytoplankton. The changes in lipid composition may then make *E. huxleyi* less palatable to *O. marina*, with wax esters being their own type of inducible chemical defense.

It is also possible that populations of strain 374 consist of cells that have natural lipidome differences, including their relative abundances of wax esters. *O. marina* engulfs its prey, and during engulfment it can sense how palatable the prey is. *E. huxleyi* with larger amounts of wax esters present in the cell membrane could be less palatable to *O. marina* than *E. huxleyi* with lower amounts of wax esters. Previous research has shown that zooplankton can sense unpalatable and/or toxic substances in prey, and selectively consume prey with lower levels of unpalatable or toxic compounds (Brown et al., 2021). Thus, through selectively grazing only on *E. huxleyi* cells with lower wax ester levels, *O. marina* predation could be driving the increase in wax esters in strain 374.

These two hypotheses which aim to explain the increase in wax esters; reorganization of the *E. huxleyi* membrane in response to grazing stress vs. selective grazing by *O. marina*, are not mutually exclusive. Indeed, it is likely that the increase of wax esters observed in strain 374 upon grazing, and many of the other lipid class changes observed in *E. huxleyi* under grazing stress, are a combined result of lipid remodeling in response to stress and selective grazing by *O. marina*. In order to parse apart these causes and effects, however, further experimental work would be needed.

Notably, the most prominent lipid classes for grazer exposed naked strain 379, which experienced the highest grazing pressure out of all the strains, do not contain wax esters. This could be due to the fact that strain 379 is motile, and a large accumulation of wax esters in and on the cell membrane might impede motility. In addition, along with motility comes the ability to evade predators, which could limit the ability of *O. marina* to engage in selective grazing of cells with low wax ester content. However, given the high rate at which 379 was consumed, this hypothesis is unlikely. Interestingly, instead of the wax esters seen accumulating in strain 374,

strain 379 sees a large increase in phospholipids PC, PG, and PA, indicating that in this strain, the depletion of DGDG lipids for TAG production is accompanied by an increase in other phospholipids.

In addition to the increase in membrane lipids discussed above, 379 grazer-exposed lipidomes contain one notable lipid, astaxanthin. This red pigment lipid has been extremely well studied due to its numerous commercial applications (Ambati et al., 2014). Astaxanthin is produced by phytoplankton and certain types of bacteria when experiencing environmental stressors such as low pH and high light intensity, and the art of finding the stressors that cause different organisms to produce maximum amounts of this lipid is a very active field of research (Hwang et al., 2019). All four strains of *E. huxleyi* in my analysis produced astaxanthin in both an ungrazed and grazed state, however the difference in production between an ungrazed and grazed state appears to be strain dependent. On average, strains 374 and 624 lipidomes increased in astaxanthin abundance upon grazing, while strain 607 decreased in astaxanthin abundance due to grazing. Strain 379 was the only strain which recorded a very large increase in production upon grazing, with an average $\log_2$ fold change of 7.64 between an ungrazed vs. grazed state. Because astaxanthin is a lipid found to be created due to environmental stress, strain 379's large increase could be due to this strain experiencing the strongest grazing pressure out of the four *E. huxleyi* strains (Harvey et al., 2015). Indeed, strain 607 experienced the least grazing pressure out of all four strains, and this strain had decreased astaxanthin production in a grazed state when compared to an ungrazed state. Studies have found that the amount of astaxanthin produced by phytoplankton is dependent upon the type and amount of stress an organism experiences (Hwang et al., 2019), so it is possible that grazing pressure is correlated with astaxanthin production in *E. huxleyi*. More research would be needed to determine whether this is the case.

Another unique lipidomic response to grazing is the increase in FFAs seen in strain 624. The presence of FFAs was not seen in the other three individual strains nor the combined strain analysis in a grazed state. Interestingly, it has been found that some free fatty acids can have inhibitory effects on the growth of other marine organisms by interfering with biochemical processes and damaging cell structures (Wu et al., 2006). For instance, certain fatty acids in cyanobacteria have been found to inhibit the growth of some types of green algae (Ikawa et al., 1996), and other fatty acids in cyanobacteria have been found to have antibacterial properties (Mundt et al., 2003). Interestingly, certain fatty acids have also been found to act as a defense against grazers in diatoms, with 5,8,11,14,17-eicosapentaenoic acid being found to be a cause of diatom biofilm toxicity to grazers (Juttner, 2001). Strain 624 experienced low grazing pressure, with *O. marina* experiencing a low growth rate despite consuming strain 624 cells at a rate comparable to the other strains. One possible reason for this low growth rate upon consuming strain 624 is that the FFAs present in strain 624 in a grazed state inhibit the growth of *O. marina* in some way, perhaps by interrupting certain biochemical pathways in *O. marina* cells.

AIM III: The *O. marina* lipidome has both shared and unique responses to feeding on different *E. huxleyi* strains

This analysis found that how the *O. marina* lipidome changes in response to feeding on different *E. huxleyi* strains is largely similar for strains 374, 379, and 624, with some striking differences arising upon consumption of strain 607. oPLS-DAs were performed which compared the lipidomes of unfed *O. marina* vs. *O. marina* fed each of the four *E. huxleyi* strains, which provided data used to uncover prominent lipid classes and individual lipid biomarkers indicative of consuming one or more specific strains. While this analysis did not reveal any individual lipid biomarkers indicative of consuming specific strains of *E. huxleyi*, there was one individual lipid,

PC 44:12 +4O, and two prominent lipid classes, TAGs and PCs, which were indicative of an overall fed state in *O. marina*. In addition, there was one lipid class, wax esters, which appeared to be indicative of a fed state in *O. marina* only after consuming strain 607.

The abundance of TAGs in *O. marina* after consuming each of the four *E. huxleyi* strains is well-supported by the literature. Marine zooplankton consist of four main types of storage lipids. These are TAGs, wax esters, phospholipids, and diacylglycerol ethers (Lee et al., 2006). TAGs are the most prominent storage lipid in terrestrial animals, and the same has been found to be true of many zooplankton species as well, where an abundance of TAGs is typically indicative of recent food consumption (Lee et al., 2006).

A recent study of the transcriptomic response of *O. marina* to starvation and feeding lends further support to the results of my aim III analysis. Transcripts found to be upregulated in response to feeding were involved in the synthesis of fatty acids and storage carbohydrates, cytoskeleton rearrangement and changes in cell shape, the detection of prey and increases in movement (Rubin et al., 2019). These results suggest that in response to feeding, *O. marina* cells process their food and create fatty acids and carbohydrates to store consumed energy, alter their cell shape and size, and increase their movement and activate different sensory channels that help them sense prey. In this way, the increase in TAGs present in *O. marina* after consuming each of the four *E. huxleyi* strains can be explained by the fact that FFAs are created to store energy after food consumption, and TAGs are created through the linkage of three fatty acids with a glycerol molecule. When fed, *O. marina* creates FFAs, many of which are converted into TAGs. Over a period of starvation, these TAGs are used for energy, which explains the reduction in TAGs present in the oPLS-DA loadings for the unfed *O. marina* in my analysis. This also could explain the DAG lipid present in *O. marina* after consuming all four strains of *E. huxleyi*,

as diglycerides are created when two fatty acids bond to a glycerol molecule. PC lipids are created using a similar biochemical pathway as DAG (Lu et al., 2020), which could explain the increase in PC lipids seen in *O. marina* after grazing. PC, being a phospholipid, could also be increasing in quantity due to the increases in membrane size that occur in response to the increased cell division that accompanies a fed state in *O. marina* (Rubin et al., 2019), although direct evidence of this is lacking.

While the *O. marina* lipid classes most indicative of the consumption of strains 374, 379, and 624 did contain one or two wax esters each, most of the lipids indicative of a fed state were TAGs. In the breakdown of the *O. marina* lipid classes most indicative of the consumption of strain 607, most of the storage lipids present were wax esters. TAGs are the predominant form of storage lipid in many zooplankton species, but in others, specifically those which are present in deep waters and/or high latitudes, wax esters are the most prominent storage lipid (Lee et al., 2006). In zooplankton, TAGs are found to be indicative of recent food consumption and are broken down more quickly for energy than wax esters, which are used for more long-term energy storage (Lee et al., 2006; Roohani et al., 2019). *E. huxleyi* strain 607 experienced the lowest grazing pressure, and *O. marina* had a negative growth rate when consuming this strain, with some *O. marina* dying (Harvey et al., 2015). It is possible that something about *E. huxleyi* strain 607 makes it toxic and/or extremely difficult to digest in some way, meaning very little of the *E. huxleyi* consumed can be digested and stored as energy by *O. marina*.

It has been suggested that *O. marina* will create wax esters during periods of low prey abundance (Roohani et al., 2019). While the *O. marina* grazing upon *E. huxleyi* strain 607 had a large abundance of prey, the *E. huxleyi* cells were apparently of very low nutritional quality. Sensing this low abundance of usable nutrients, the *O. marina* consuming strain 607 could have

stored much of what was consumed as wax esters, as the ability to extract energy from the food source at hand was quite low, and long-term energy storage molecules were created to enhance the probability of survival. In effect, the *O. marina* consuming strain 607 stored energy from *E. huxleyi* as though it were in an environment with low food abundance, perhaps due to the poor nutritional quality of this strain. The *O. marina* consuming the other three strains, which did seem to be of acceptable nutritional quality, might have stored most of the energy consumed as TAGs because they sensed a suitable food source was abundant.

There was only one lipid present in *O. marina* fed all strains, PC 44:12 +4O, that was also not present in the unfed *O. marina* lipidome. While this single lipid could be viewed as a potential biomarker for fed *O. marina*, we cannot claim this lipid is a biomarker for fed *O. marina* at large. Unfed *O. marina* and fed *O. marina* are not two completely divorced states; rather, they are two points along a spectrum. There are many different stages of feeding, from grazing on just enough prey for survival to gorging on a large abundance of prey. Where an unfed state begins is also somewhat arbitrary and is decided upon by the experimenter. Is it one day after eating? A week after eating? The endpoint of an unfed state, death, is clear. In this experiment, *O. marina* was considered to be in an unfed state four days after their last meal. However, the *O. marina* was by no means on the brink of death, and each cell still had varying amounts of 147 different individual lipids present. Indeed, studies have shown that during starvation, primarily wax ester stores are depleted (after TAG stores are used), while the types and ratios of different lipids present in an organism remain more or less constant (Roohani et al., 2019). In line with those findings, it seems as though in the Harvey et al. (2015) experiment, starved *O. marina* maintained the diversity of its lipidome during its period of food deprivation, while depleting the large variety of wax esters and TAGs it had in store. It is impossible to know

whether or not more time in an unfed state would lead to more lipids being absent from the starved *O. marina* lipidome, or if less time in an unfed state would have led to lipid PC 44:12 +4O being present in the unfed *O. marina* lipidome. In other words, it is very possible that PC 44:12 +4O was simply the first lipid to be completely broken down during the period of starvation that the *O. marina* in this experiment underwent. If less time had been spent in an unfed state, the lipid may still have been present in the unfed lipidome. If more time had been spent in an unfed state, there could have been more lipids absent from the unfed lipidome.

Taken together, this data suggests that while the *O. marina* lipidome reacts to feeding on different *E. huxleyi* strains in a similar way, there are numerous strain-specific differences which have the potential to impact *O. marina* growth rate. The Harvey et al. (2015) experiment found that there were differences in both *O. marina* ingestion rate and *O. marina* growth rate depending on which *E. huxleyi* strain was consumed. However, the rate at which *O. marina* ingested each *E. huxleyi* strain did not correspond to how quickly the *O. marina* grew while ingesting these strains (Table 1), indicating that consuming different *E. huxleyi* strains could lead to differences in energy storage and processing in *O. marina*. Based on the results of my aim III analysis, this hypothesis remains a distinct possibility.

CONCLUSIONS & FUTURE DIRECTIONS

My aim I analysis examined the ungrazed *E. huxleyi* lipidome, looking for variations due to calcification state and ploidy level, as well as lipids that were at relatively constant levels in all four strains. DGDGs, PGs, TAGs, and S_DGCCs were classes found to be more prominent in a naked state (Fig. 1C), with five individual lipids found to be unique to and indicative of a naked state (Table 3). Wax esters, coprostanol esters, and PDPTs were classes found to be more

prominent in a calcified state in *E. huxleyi* (Fig. 1D), with five individual lipids found to be unique to and indicative of a calcified state (Table 4). SQDGs and S_DGCCs were found to be more prominent in the haploid strain (Fig. 2B), however no individual lipids were found to be indicative of a haploid state. Wax esters and coprostanol esters were found to be more prominent in diploid strains (Fig. 2C), with 19 individual lipids found to be unique to and indicative of a diploid state. An analysis of lipids common to all four *E. huxleyi* strains revealed that 67% of *E. huxleyi* lipids are shared by all four strains in an ungrazed state (Fig. 3B). Of these 185 shared lipids, 22 were found to be largely unchanging due to calcification state and ploidy level (Table 6). Overall, my aim I analysis found numerous lipid classes and individual lipids that are indicative of various states in ungrazed *E. huxleyi*. This indicates that the lipidomes of the four *E. huxleyi* strains in this analysis have both a core lipidome that is common between them, as well as numerous differences which make the lipidome of each strain unique.

My aim II analysis examined the *E. huxleyi* lipidome of each individual strain, as well as all four combined strains, in response to grazing. The main finding of this analysis was that the *E. huxleyi* lipidome reacts to grazing in a very strain-specific way. There were numerous lipids and lipid classes found to be indicative of each specific strain in a grazed state, as identified by PCA analysis (Figs. 4E-H). In strain 374, wax esters and coprostanol esters were found to become more prominent after grazing. Strain 379 saw a large increase in astaxanthin, PGs, and PCs. Strain 607 experienced an increase in PGs and PCs. Strain 624 had increases in FFAs and coprostanol esters. The analysis which compared all four *E. huxleyi* strains in an ungrazed vs. grazed state (Fig. 5D,E) revealed that increases in TAGs, coprostanol esters, and PCs are indicative of an overall grazed state in *E. huxleyi*. There were also 19 lipids identified which were found to be unique and indicative to a grazed state in all four *E. huxleyi* strains (Table 7).

The results of this aim II analysis indicate that some lipid classes, such as TAGs, increase in all four *E. huxleyi* strains upon exposure to grazing pressure, while other lipid classes and individual lipids change in response to grazing in a very strain specific way.

In my aim III analysis, the response of the *O. marina* lipidome to feeding on each individual *E. huxleyi* strain was explored. The results of this analysis showed that the *O. marina* lipidome responded to grazing in a very similar way when consuming all four strains (Figs. 6E-H), with large increases in TAGs found to be indicative of a fed state, along with a suite of other lipid classes. The *O. marina* lipidome after feeding on strain 607 differed from that of the other three strains in one notable way, with *O. marina* experiencing a large increase in wax esters after grazing on this strain (Fig. 6G). Since the growth rate of *O. marina* was negative while consuming strain 607 (Table 1), this result is exciting and ripe for future analysis. Overall, these results show us that the *O. marina* lipidome reacts to feeding in a very similar way, regardless of strain identity. The results also indicate that wax esters, found to be prominent in the *O. marina* lipidome after feeding on strain 607, may be indicative of consuming a toxic or non-nutritious food source.

For this thesis, I relied heavily on principal component analysis and presence/absence analysis to find individual lipids and lipid classes which are indicative of certain strains and states in *E. huxleyi* and *O. marina*. However, there are many other types of analysis that can be performed with lipidomics datasets. One such analysis, PLSR (partial least squares regression) has the potential to identify correlations between lipidomes and other variables, such as *O. marina* growth rate as measured in the Harvey et al. (2015) experiment. Using a Solo software program, I performed three preliminary PLSR analyses which compared *O. marina* growth rate to all four *E. huxleyi* control lipidomes, all four *E. huxleyi* grazed lipidomes, and *O. marina*

lipidomes after grazing on all four strains. Of these three PLSRs, the comparison between *O. marina* growth rate and the *O. marina* grazed lipidome seemed quite promising and will be further explored. This future work is performed in recognition of the fact that the lipidome of an organism is both a reflection of the state and experiences of that organism, as well as a variable that will impact the behavior and lipidome of the predators that consume that organism. The lipidome of a phytoplankton or zooplankton can have an impact on top-of-the-food-chain predators, and the future examination of *E. huxleyi* and *O. marina* lipidomes and their correlation with *O. marina* grazing behavior and growth rate, brings us one small step closer to understanding this incredibly complex interplay between biomolecule composition and predation.

It is useful to note that while changes in the lipidome are only one of many ways to investigate the predator-prey dynamic between *E. huxleyi* and *O. marina*, they have a number of advantages that other bioinformatic tools lack. While a similar analysis could have been performed which examined changes in the transcriptomes or proteomes of *E. huxleyi* and *O. marina* under different states and in response to grazing, the lipid makeup of these organisms could only be loosely estimated at best. There are numerous ways in which lipid-building enzymes are regulated post-transcriptionally, and many lipids can be in varying states of breakdown or synthesis that cannot be predicted from the transcriptome or proteome alone. The nuances of these changes, and the absolute values of different types of lipids present, would be lost with other types of bioinformatic analysis. A very useful approach for future lipidomics work may be to combine different bioinformatic analyses. For instance, one could perform both a lipidomic and transcriptomic analysis on a set of samples. This would provide information about which genes were active in an organism in a certain state or treatment, as well as the type and

quantity of lipids created from these gene products. In addition to information on the lipidome, this type of combined analysis would provide a host of additional information regarding the proteins, RNAs, and other biomolecules present in cells in certain states and undergoing different treatments.

Taken together, the results of my three aims indicate that lipidomics analysis can be a useful tool when studying different states in *E. huxleyi* and *O. marina*. While the lipidome itself may not be sufficient to concretely identify different strains and states, the changes observed in this analysis provide insight into the internal functioning of these organisms under different growth conditions. Lipidomic analysis is uniquely suited to the study of grazing interactions for several reasons. First, because lipids make up the membranes of *E. huxleyi* cells, they are the first molecules that *O. marina* encounters upon physical contact. Thus, changes in this lipid bilayer makeup could lead to selective grazing by *O. marina*. Second, lipids are much more concentrated sources of energy than carbohydrates or protein and are widely known to influence predators' perceived palatability of prey. In addition, the amount and type of lipids present in prey are known to influence the health and growth potential of predators. Therefore, the overall lipid makeup of *E. huxleyi* could have a larger influence on *O. marina* growth rate than the makeup of carbohydrates or proteins. Third, the ability of the lipidome to change in response to stress is well known. Therefore, the changes seen in the *E. huxleyi* lipidome due to grazing pressure, and the changes in the *O. marina* lipidome in response to consuming strain 607, provide windows into how these organisms respond to stress. Considering the role of phytoplankton in the marine food web as well as global cycling, and how grazing by protists is one of the largest top-down controls on phytoplankton populations, understanding how the lipidomes of grazers and their prey influence each other is incredibly important.

References

Ambati, R. R., Phang, S.-M., Ravi, S., & Aswathanarayana, R. G. (2014). Astaxanthin: Sources, Extraction, Stability, Biological Activities and Its Commercial Applications—A Review. *Marine Drugs*, *12*(1), 128–152. https://doi.org/10.3390/md12010128

Arteaga, L. A., Boss, E., Behrenfeld, M. J., Westberry, T. K., & Sarmiento, J. L. (2020). Seasonal modulation of phytoplankton biomass in the Southern Ocean. *Nature Communications*, *11*(1), 5364. https://doi.org/10.1038/s41467-020-19157-2

Aveiro, S. S., Melo, T., Figueiredo, A., Domingues, P., Pereira, H., Maia, I. B., Silva, J., Domingues, M. R., Nunes, C., & Moreira, A. S. P. (2020). The Polar Lipidome of Cultured *Emiliania huxleyi*: A Source of Bioactive Lipids with Relevance for Biotechnological Applications. *Biomolecules*, *10*(10), 1434. https://doi.org/10.3390/biom10101434

Brett, M., & Müller-Navarra, D. (1997). The role of highly unsaturated fatty acids in aquatic foodweb processes. *Freshwater Biology*, *38*(3), 483–499. https://doi.org/10.1046/j.1365-2427.1997.00220.x

Brown, E. R., & Kubanek, J. (2020). Harmful alga trades off growth and toxicity in response to cues from dead phytoplankton. *Limnology and Oceanography*, *65*(8), 1723–1733. https://doi.org/10.1002/lno.11414

Brown, E. R., Moore, S. G., Gaul, D. A., & Kubanek, J. (2021). Differentiating toxic and nontoxic congeneric harmful algae using the non-polar metabolome. *Harmful Algae*, *110*, 102129. https://doi.org/10.1016/j.hal.2021.102129

Brownlee, C., Wheeler, G. L., & Taylor, A. R. (2015). Coccolithophore biomineralization: New questions, new answers. *Seminars in Cell & Developmental Biology*, *46*, 11–16. https://doi.org/10.1016/j.semcdb.2015.10.027

Calbet, A., Isari, S., Martínez, R., Saiz, E., Garrido, S., Peters, J., Borrat, R., & Alcaraz, M. (2013). Adaptations to feast and famine in different strains of the marine heterotrophic dinoflagellates Gyrodinium dominans and Oxyrrhis marina. *Marine Ecology Progress Series*, *483*, 67–84. https://doi.org/10.3354/meps10291

Calbet, A., & Landry, M. R. (2004). Phytoplankton growth, microzooplankton grazing, and carbon cycling in marine systems. *Limnology and Oceanography*, *49*(1), 51–57. https://doi.org/10.4319/lo.2004.49.1.0051

Collins, J. R., Edwards, B. R., Fredricks, H. F., & Van Mooy, B. A. S. (2016). LOBSTAHS: An Adduct-Based Lipidomics Strategy for Discovery and Identification of Oxidative Stress Biomarkers. *Analytical Chemistry*, *88*(14), 7154–7162. https://doi.org/10.1021/acs.analchem.6b01260

Dairi, T., Kuzuyama, T., Nishiyama, M., & Fujii, I. (2011). Convergent strategies in biosynthesis. *Natural Product Reports*, *28*(6), 1054–1086. https://doi.org/10.1039/C0NP00047G

Eltgroth, M. L., Watwood, R. L., & Wolfe, G. V. (2005). PRODUCTION AND CELLULAR LOCALIZATION OF NEUTRAL LONG-CHAIN LIPIDS IN THE HAPTOPHYTE ALGAE ISOCHRYSIS GALBANA AND *EMILIANIA HUXLEYI*. *Journal of Phycology*, *41*(5), 1000–1009. https://doi.org/10.1111/j.1529-8817.2005.00128.x

Field, C. B., Behrenfeld, M. J., Randerson, J. T., & Falkowski, P. (1998). Primary Production of the Biosphere: Integrating Terrestrial and Oceanic Components. *Science*, *281*(5374), 237–240. https://doi.org/10.1126/science.281.5374.237

Frada, M., Probert, I., Allen, M. J., Wilson, W. H., & de Vargas, C. (2008). The "Cheshire Cat" escape strategy of the coccolithophore *Emiliania huxleyi* in response to viral infection. *Proceedings of the National Academy of Sciences*, *105*(41), 15944–15949. https://doi.org/10.1073/pnas.0807707105

Fulton, J. M., Fredricks, H. F., Bidle, K. D., Vardi, A., Kendrick, B. J., DiTullio, G. R., & Van Mooy, B. A. S. (2014). Novel molecular determinants of viral susceptibility and resistance in the lipidome of *E miliania huxleyi*: Novel lipids in *Emiliania huxleyi*. *Environmental Microbiology*, *16*(4), 1137–1149. https://doi.org/10.1111/1462-2920.12358

Gordillo, F. J. L., Goutx, M., Figueroa, F. L., & Niell, F. X. (1998). Effects of light intensity, CO2 and nitrogen supply on lipid class composition of Dunaliella viridis. *Journal of Applied Phycology*, *10*(2), 135–144. https://doi.org/10.1023/A:1008067022973

Harvey, E. L., Bidle, K. D., & Johnson, M. D. (2015). Consequences of strain variability and calcification in *Emiliania huxleyi* on microzooplankton grazing. *Journal of Plankton Research*, fbv081. https://doi.org/10.1093/plankt/fbv081

Haunost, M., Riebesell, U., & Bach, L. T. (2020). The Calcium Carbonate Shell of *Emiliania huxleyi* Provides Limited Protection Against Viral Infection. *Frontiers in Marine Science*, *7*. https://www.frontiersin.org/article/10.3389/fmars.2020.530757

Henriksen, K., Young, J. R., Bown, P. R., & Stipp, S. L. S. (2004). Coccolith biomineralisation studied with atomic force microscopy. *Palaeontology*, *47*(3), 725–743. https://doi.org/10.1111/j.0031-0239.2004.00385.x

Huang, B., Marchand, J., Thiriet-Rupert, S., Carrier, G., Saint-Jean, B., Lukomska, E., Moreau, B., Morant-Manceau, A., Bougaran, G., & Mimouni, V. (2019). Betaine lipid and neutral lipid production under nitrogen or phosphorus limitation in the marine microalga Tisochrysis lutea (Haptophyta). *Algal Research*, *40*, 101506. https://doi.org/10.1016/j.algal.2019.101506

Hunter, J. E., Frada, M. J., Fredricks, H. F., Vardi, A., & Van Mooy, B. A. S. (2015). Targeted and untargeted lipidomics of *Emiliania huxleyi* viral infection and life cycle phases highlights molecular biomarkers of infection, susceptibility, and ploidy. *Frontiers in Marine Science*, *2*. https://www.frontiersin.org/article/10.3389/fmars.2015.00081

Hwang, S.-W., Choi, H. I., & Sim, S. J. (2019). Acidic cultivation of Haematococcus pluvialis for improved astaxanthin production in the presence of a lethal fungus. *Bioresource Technology*, *278*, 138–144. https://doi.org/10.1016/j.biortech.2019.01.080

Ikawa, M., Haney, J. F., & Sasner, J. J. (1996). Inhibition of Chlorella growth by the lipids of cyanobacterium Microcystis aeruginosa. *Hydrobiologia*, *331*(1), 167–170. https://doi.org/10.1007/BF00025418

Jónasdóttir, S. H. (2019). Fatty Acid Profiles and Production in Marine Phytoplankton. *Marine Drugs*, *17*(3), 151. https://doi.org/10.3390/md17030151

Juttner, F. (2001). LIBERATION OF 5,8,11,14,17-EICOSAPENTAENOIC ACID AND OTHER POLYUNSATURATED FATTY ACIDS FROM LIPIDS AS A GRAZER DEFENSE REACTION IN EPILITHIC DIATOM BIOFILMS. *Journal of Phycology*, *37*(5), 744–755. https://doi.org/10.1046/j.1529-8817.2001.00130.x

Lee, R., Hagen, W., & Kattner, G. (2006). Lipid storage in marine zooplankton. *Marine Ecology Progress Series*, *307*, 273–306. https://doi.org/10.3354/meps307273

Li, F., Wu, X., Lam, P., Bird, D., Zheng, H., Samuels, L., Jetter, R., & Kunst, L. (2008). Identification of the Wax Ester Synthase/Acyl-Coenzyme A:Diacylglycerol Acyltransferase WSD1 Required for Stem Wax Ester Biosynthesis in Arabidopsis. *Plant Physiology*, *148*(1), 97–107. https://doi.org/10.1104/pp.108.123471

Lowe, C. D., Keeling, P. J., Martin, L. E., Slamovits, C. H., Watts, P. C., & Montagnes, D. J. S. (2011). Who is *Oxyrrhis marina*? Morphological and phylogenetic studies on an unusual dinoflagellate. *Journal of Plankton Research*, *33*(4), 555–567. https://doi.org/10.1093/plankt/fbq110

Lu, J., Xu, Y., Wang, J., Singer, S. D., & Chen, G. (2020). The Role of Triacylglycerol in Plant Stress Response. *Plants*, *9*(4), 472. https://doi.org/10.3390/plants9040472

Mackinder, L., Wheeler, G., Schroeder, D., Riebesell, U., & Brownlee, C. (2010). Molecular Mechanisms Underlying Calcification in Coccolithophores. *Geomicrobiology Journal*, *27*(6–7), 585–595. https://doi.org/10.1080/01490451003703014

Maeda, Y., Nojima, D., Yoshino, T., & Tanaka, T. (2017). Structure and properties of oil bodies in diatoms. *Philosophical Transactions of the Royal Society B: Biological Sciences*, *372*(1728), 20160408. https://doi.org/10.1098/rstb.2016.0408

Matson, P. G., Ladd, T. M., Halewood, E. R., Sangodkar, R. P., Chmelka, B. F., & Iglesias-Rodriguez, M. D. (2016). Intraspecific Differences in Biogeochemical Responses to Thermal Change in the Coccolithophore *Emiliania huxleyi*. *PLOS ONE*, *11*(9), e0162313. https://doi.org/10.1371/journal.pone.0162313

Mayers, K. M. J., Poulton, A. J., Bidle, K., Thamatrakoln, K., Schieler, B., Giering, S. L. C., Wells, S. R., Tarran, G. A., Mayor, D., Johnson, M., Riebesell, U., Larsen, A., Vardi, A., & Harvey, E. L. (2020). The Possession of Coccoliths Fails to Deter Microzooplankton Grazers. *Frontiers in Marine Science*, *7*. https://www.frontiersin.org/article/10.3389/fmars.2020.569896

MetaboAnalyst. (n.d.). Retrieved April 9, 2022, from https://www.metaboanalyst.ca/home.xhtml

Monteiro, F. M., Bach, L. T., Brownlee, C., Bown, P., Rickaby, R. E. M., Poulton, A. J., Tyrrell, T., Beaufort, L., Dutkiewicz, S., Gibbs, S., Gutowska, M. A., Lee, R., Riebesell, U., Young, J., & Ridgwell, A. (2016). Why marine phytoplankton calcify. *Science Advances*, *2*(7), e1501822. https://doi.org/10.1126/sciadv.1501822

Mundt, S., Kreitlow, S., & Jansen, R. (2003). Fatty acids with antibacterial activity from the cyanobacterium Oscillatoria redekei HUB 051. *Journal of Applied Phycology*, *15*(2), 263–267. https://doi.org/10.1023/A:1023889813697

Murakami, H., Nobusawa, T., Hori, K., Shimojima, M., & Ohta, H. (2018). Betaine Lipid Is Crucial for Adapting to Low Temperature and Phosphate Deficiency in Nannochloropsis1[OPEN]. *Plant Physiology*, *177*(1), 181–193. https://doi.org/10.1104/pp.17.01573

Pan, Y.-J., Sadovskaya, I., Hwang, J.-S., & Souissi, S. (2018). Assessment of the fecundity, population growth and fatty acid composition of *Apocyclops royi* (Cyclopoida, Copepoda) fed on different microalgal diets. *Aquaculture Nutrition*, *24*(3), 970–978. https://doi.org/10.1111/anu.12633

Patwari, P., Salewski, V., Gutbrod, K., Kreszies, T., Dresen-Scholz, B., Peisker, H., Steiner, U., Meyer, A. J., Schreiber, L., & Dörmann, P. (2019). Surface wax esters contribute to drought tolerance in Arabidopsis. *The Plant Journal*, *98*(4), 727–744. https://doi.org/10.1111/tpj.14269

Piepho, M., Martin-Creuzburg, D., & Wacker, A. (2010). Simultaneous Effects of Light Intensity and Phosphorus Supply on the Sterol Content of Phytoplankton. *PLOS ONE*, *5*(12), e15828. https://doi.org/10.1371/journal.pone.0015828

Piironen, V., Lindsay, D. G., Miettinen, T. A., Toivo, J., & Lampi, A.-M. (2000). Plant sterols: biosynthesis, biological function and their importance to human nutrition. *Journal of the Science of Food and Agriculture*, *80*(7), 939–966. https://doi.org/10.1002/(SICI)1097-0010(20000515)80:7<939::AID-JSFA644>3.0.CO;2-C

Poulin, R. X., Lavoie, S., Siegel, K., Gaul, D. A., Weissburg, M. J., & Kubanek, J. (2018). Chemical encoding of risk perception and predator detection among estuarine invertebrates. *Proceedings of the National Academy of Sciences*, *115*(4), 662–667. https://doi.org/10.1073/pnas.1713901115

Poulson-Ellestad, K. L., Harvey, E. L., Johnson, M. D., & Mincer, T. J. (2016). Evidence for Strain-Specific Exometabolomic Responses of the Coccolithophore *Emiliania huxleyi* to Grazing by the Dinoflagellate *Oxyrrhis marina*. *Frontiers in Marine Science*, *3*. https://www.frontiersin.org/article/10.3389/fmars.2016.00001

Rasdi, N. W., Qin, J. G., & Li, Y. (2016). Effects of dietary microalgae on fatty acids and digestive enzymes in copepod *Cyclopina kasignete* , a potential live food for fish larvae. *Aquaculture Research*, *47*(10), 3254–3264. https://doi.org/10.1111/are.12778

Ribalet, F., Bastianini, M., Vidoudez, C., Acri, F., Berges, J., Ianora, A., Miralto, A., Pohnert, G., Romano, G., Wichard, T., & Casotti, R. (2014). Phytoplankton Cell Lysis Associated with Polyunsaturated Aldehyde Release in the Northern Adriatic Sea. *PLoS ONE*, *9*(1), e85947. https://doi.org/10.1371/journal.pone.0085947

Roberts, E. C., Wootton, E. C., Davidson, K., Jeong, H. J., Lowe, C. D., & Montagnes, D. J. S. (2011). Feeding in the dinoflagellate *Oxyrrhis marina*: linking behaviour with mechanisms. *Journal of Plankton Research*, *33*(4), 603–614. https://doi.org/10.1093/plankt/fbq118

Roohani, K., Haubrich, B. A., Yue, K.-L., D'Souza, N., Montalbano, A., Rynearson, T., Menden-Deuer, S., & Reid, C. W. (2019). Trophic upgrading and mobilization of wax esters in microzooplankton. *PeerJ*, *7*, e7549. https://doi.org/10.7717/peerj.7549

Rubin, E. T., Cheng, S., Montalbano, A. L., Menden-Deuer, S., & Rynearson, T. A. (2019). Transcriptomic Response to Feeding and Starvation in a Herbivorous Dinoflagellate. *Frontiers in Marine Science*, *6*. https://www.frontiersin.org/article/10.3389/fmars.2019.00246

Sargent, J. R., Gatten, R. R., & McIntosh, R. (1977). Wax esters in the marine environment — their occurrence, formation, transformation and ultimate fates. *Marine Chemistry*, *5*(4), 573–584. https://doi.org/10.1016/0304-4203(77)90043-3

Sayanova, O., Mimouni, V., Ulmann, L., Morant-Manceau, A., Pasquet, V., Schoefs, B., & Napier, J. A. (2017). Modulation of lipid biosynthesis by stress in diatoms. *Philosophical Transactions of the Royal Society B: Biological Sciences*, *372*(1728), 20160407. https://doi.org/10.1098/rstb.2016.0407

Selander, E., Kubanek, J., Hamberg, M., Andersson, M. X., Cervin, G., & Pavia, H. (2015). Predator lipids induce paralytic shellfish toxins in bloom-forming algae. *Proceedings of the National Academy of Sciences*, *112*(20), 6395–6400. https://doi.org/10.1073/pnas.1420154112

Sheyn, U., Rosenwasser, S., Lehahn, Y., Barak-Gavish, N., Rotkopf, R., Bidle, K. D., Koren, I., Schatz, D., & Vardi, A. (2018). Expression profiling of host and virus during a coccolithophore bloom provides insights into the role of viral infection in promoting carbon export. *The ISME Journal*, *12*(3), 704–713. https://doi.org/10.1038/s41396-017-0004-x

Strom, S. L., Bright, K. J., Fredrickson, K. A., & Cooney, E. C. (2018). Phytoplankton defenses: Do *Emiliania huxleyi* coccoliths protect against microzooplankton predators? *Limnology and Oceanography*, *63*(2), 617–627. https://doi.org/10.1002/lno.10655

Taylor, A. R., Brownlee, C., & Wheeler, G. (2017). Coccolithophore Cell Biology: Chalking Up Progress. *Annual Review of Marine Science*, *9*(1), 283–310. https://doi.org/10.1146/annurev-marine-122414-034032

Triantaphyllou, M., Dimiza, M., Krasakopoulou, E., Malinverno, E., Lianou, V., & Souvermezoglou, E. (2010). Seasonal variation in *Emiliania huxleyi* coccolith morphology and calcification in the Aegean Sea (Eastern Mediterranean). *Geobios*, *43*(1), 99–110. https://doi.org/10.1016/j.geobios.2009.09.002

Wu, J.-T., Chiang, Y.-R., Huang, W.-Y., & Jane, W.-N. (2006). Cytotoxic effects of free fatty acids on phytoplankton algae and cyanobacteria. *Aquatic Toxicology*, *80*(4), 338–345. https://doi.org/10.1016/j.aquatox.2006.09.011

Young, J. R., Davis, S. A., Bown, P. R., & Mann, S. (1999). Coccolith Ultrastructure and Biomineralisation. *Journal of Structural Biology*, *126*(3), 195–215. https://doi.org/10.1006/jsbi.1999.4132

Zienkiewicz, K., Du, Z.-Y., Ma, W., Vollheyde, K., & Benning, C. (2016). Stress-induced neutral lipid biosynthesis in microalgae — Molecular, cellular and physiological insights. *Biochimica et Biophysica Acta (BBA) - Molecular and Cell Biology of Lipids*, *1861*(9, Part B), 1269–1281. https://doi.org/10.1016/j.bbalip.2016.02.008